U.S. AIR FORCE

USSF

AFRL

Long range 3D imaging with digital holography

Matthias T. Banet

Directed Energy Directorate, Air Force Research Laboratory

afrl.rdl.orgmailbox@us.af.mil

Digital holography with wavelength diversity enables 3D imaging

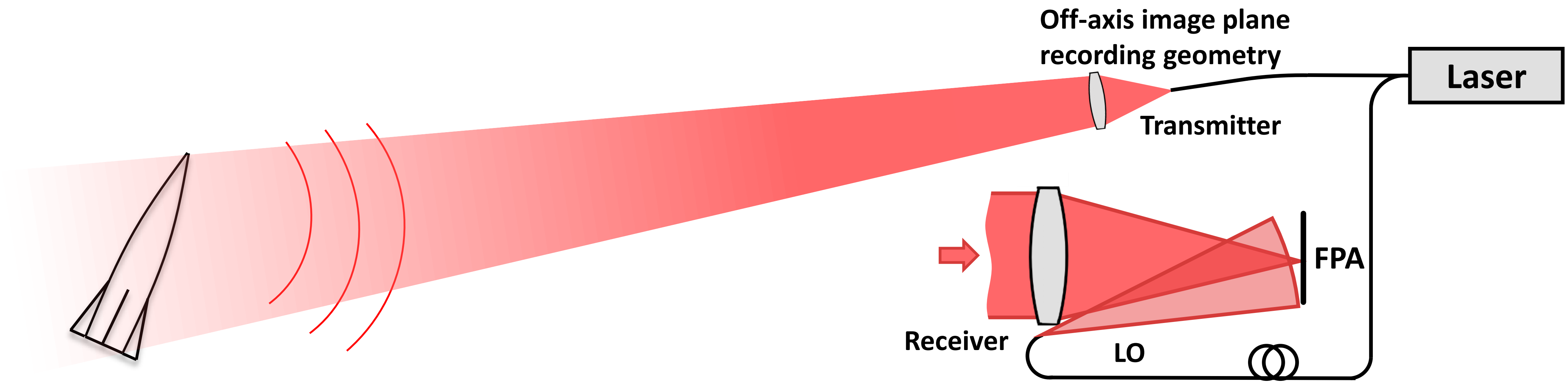

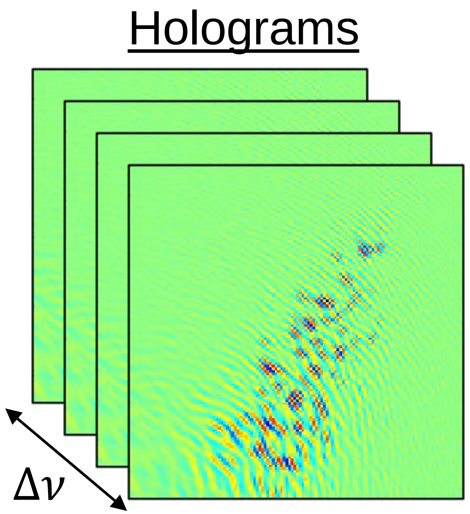

- Flood illuminate distant object with coherent light
- Interfere image of object with off-axis reference beam resulting in a hologram
- Repeat for many frequencies in a narrow bandwidth
- Perform Fourier transform over optical frequency to generate 3D image

Marron, J. C. and Schroeder, K. S., "Holographic laser radar," Opt. Lett. 18, 385–387 (Mar 1993).

Reflectance and depth profiles enable simulation of 3D imaging

Reflectance

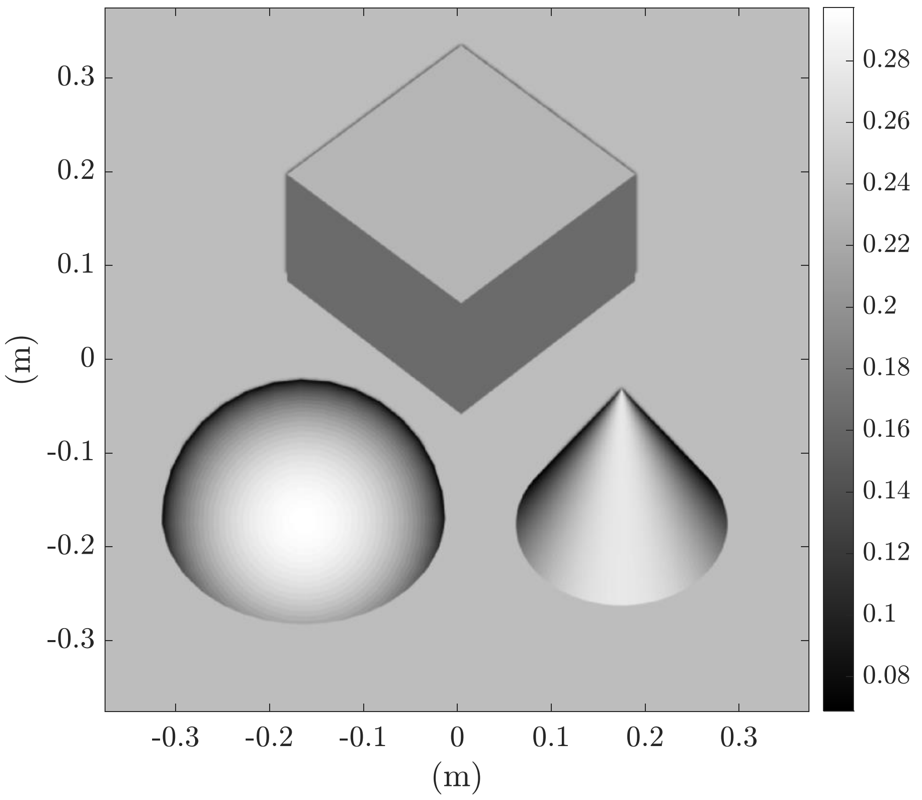

Depth

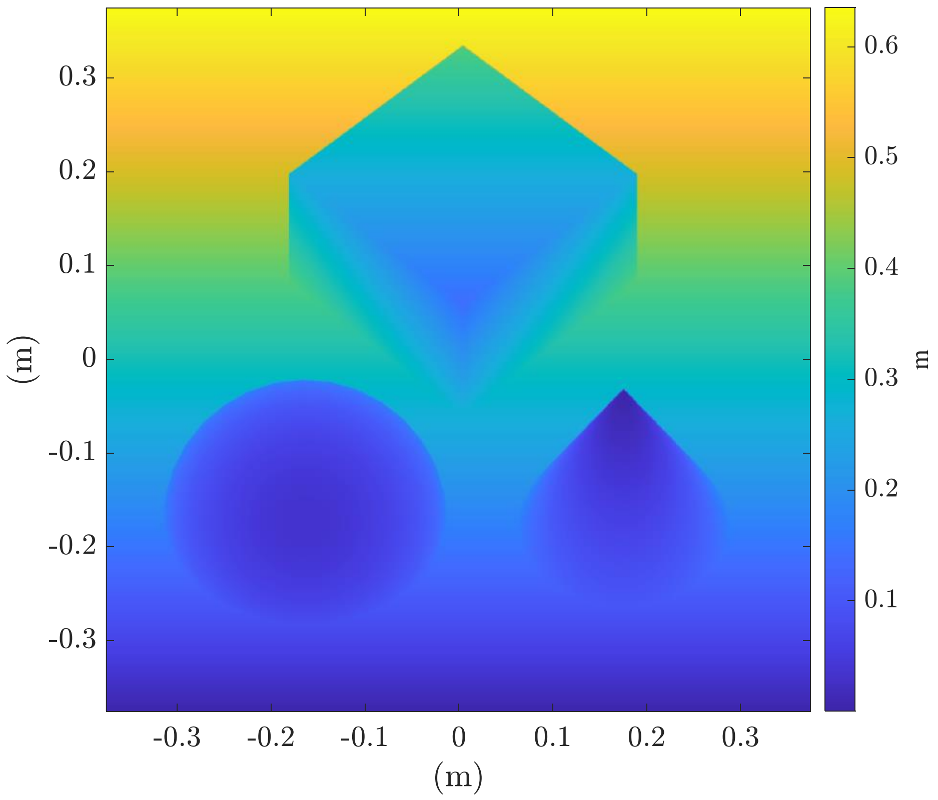

Blender Online Community, Blender - a 3D modelling and rendering package. Blender Foundation, Stichting Blender Foundation, Amsterdam (2018).

Fourier processing provides amplitude and phase estimates

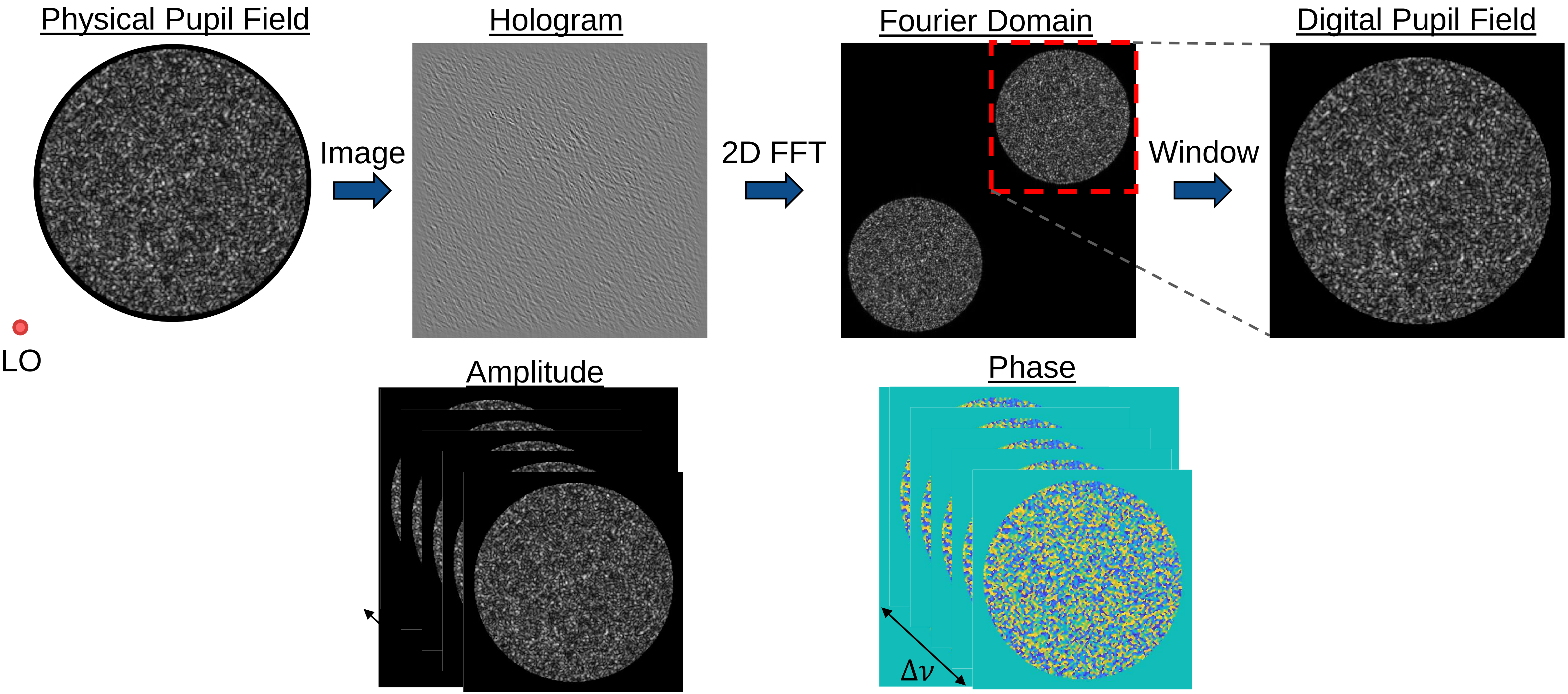

3D and range imagery after Fourier transforming complex fields

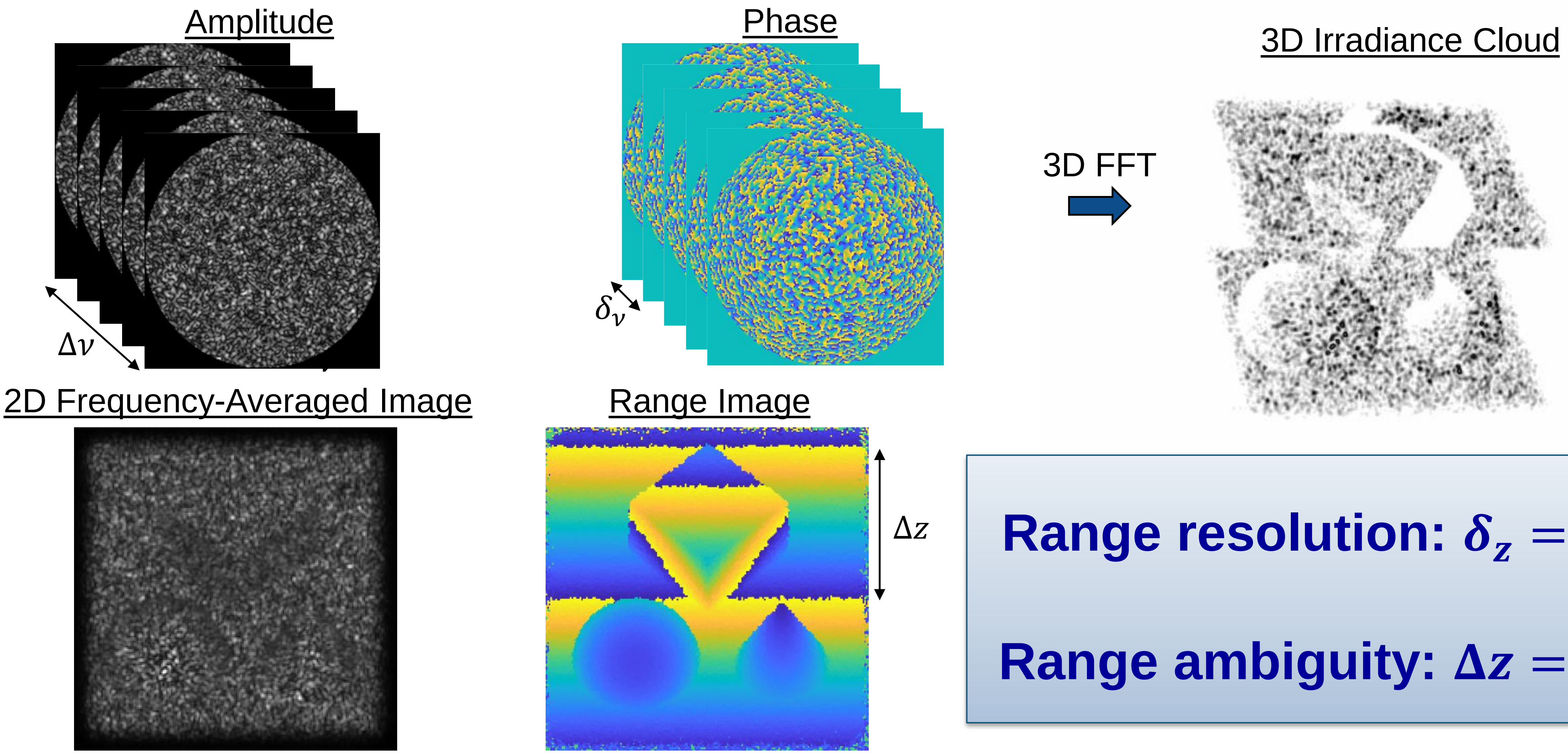

Range resolution: $\delta_z = \frac{c}{2\Delta\nu}$

Range ambiguity: $\Delta z = \frac{c}{2\delta_\nu}$

Conventional 3D imaging pulse train

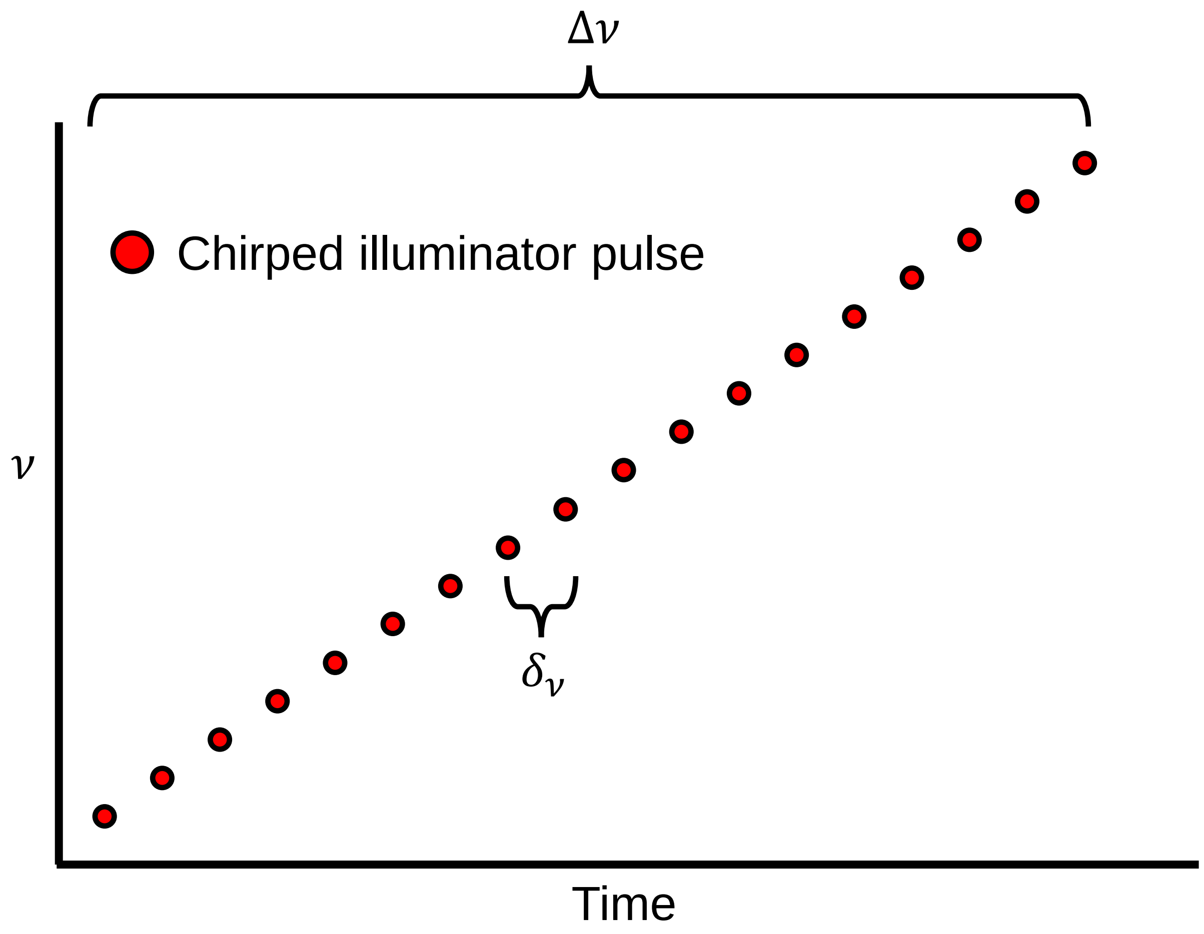

Range image

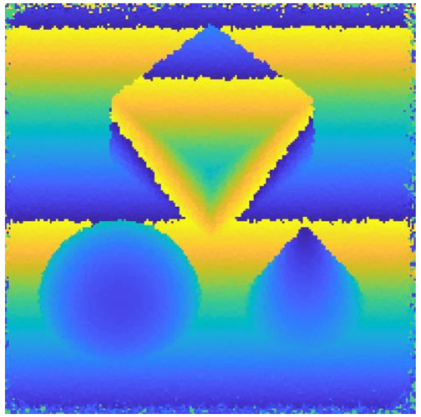

Range image formed by taking z-location of maximum irradiance in 3D image

Range resolution: $\delta_z = \frac{c}{2\Delta\nu}$

Range ambiguity: $\Delta z = \frac{c}{2\delta_\nu}$

3D imaging theory for rough, opaque objects

- Write object depth profile as

$$z_0 + Z(u,v)$$

- Write 2D coherent image of the object for some general illumination frequency, ν

$$U_i(u,v;\nu) = \exp(i4\pi\nu z_0/c) \times \underline{h(u,v)} * \{\underline{U_{0,\perp}(u,v)\exp[i4\pi\nu Z(u,v)/c]}\}$$

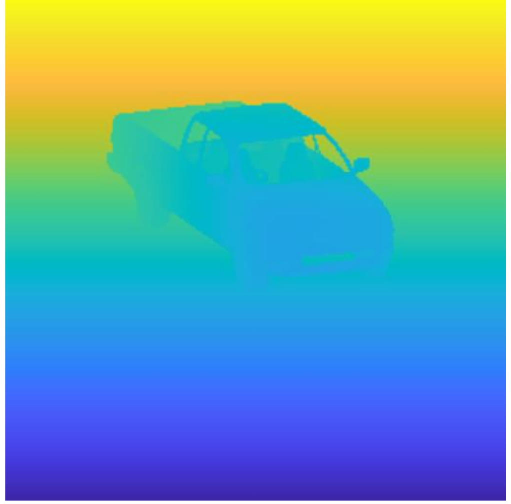

- Break up relative depth profile into coarse and rough components

$$Z(u,v) = \underline{Z_d(u,v)} + \underline{Z_r(u,v)}$$

- Rewrite 2D coherent image as

$$U_i(u,v;\nu) \approx \exp(i4\pi\nu z_0/c)\,\underline{\exp[i4\pi\nu Z_d(u,v)/c]} \times \underline{(h(u,v) * \{U_{0,\perp}(u,v)\exp[i4\pi\nu Z_r(u,v)/c]\})}$$

Causes speckle!

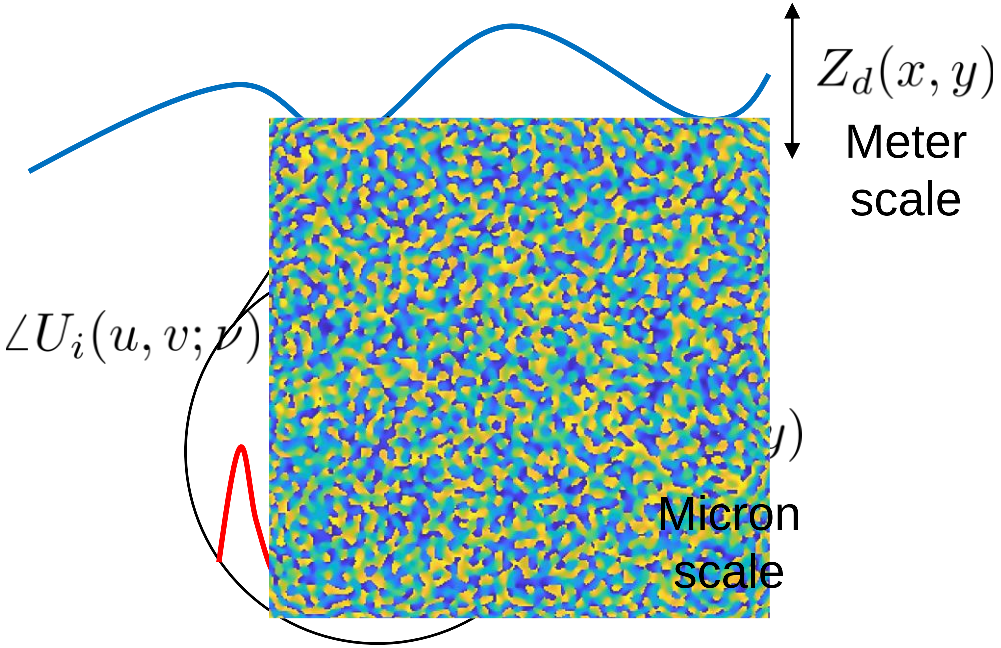

3D imaging theory for narrow illuminating bandwidths: $\delta_\nu/\nu_0 \sim 10^{-5}$

- If $Z_r(u,v)$ is constant for a sequence of illumination frequencies, ν_m

$$U_i(u,v;\nu_m) \approx \exp(i4\pi\nu_m z_0/c)\, \underline{\exp[i4\pi\nu_m Z_d(u,v)/c]} \times (h(u,v) * \{U_{0,\perp}(u,v)\, \underline{\exp[i4\pi\nu_m Z_r(u,v)/c]}\})$$

- Write ν_m as

$$\nu_m = \nu_0 + m\delta_\nu$$

- Examine pertinent phasors containing ν_m

$$\exp[i4\pi(\nu_0 + m\delta_\nu) Z_d(u,v)/c]$$

$$\exp[i4\pi(\nu_0 + m\delta_\nu) Z_r(u,v)/c] \approx \exp[i4\pi\nu_0 Z_r(u,v)/c]$$

$$U_i(u,v;\nu_m) \approx \exp[i4\pi\nu_m z_0/c]\, \underline{\exp[i4\pi\nu_m Z_d(u,v)/c]} \times (h(u,v) * \{U_{0,\perp}(u,v)\, \underline{\exp[i4\pi\nu_0 Z_r(u,v)/c]}\})$$

$\angle U_i(u,v;\nu_m)$

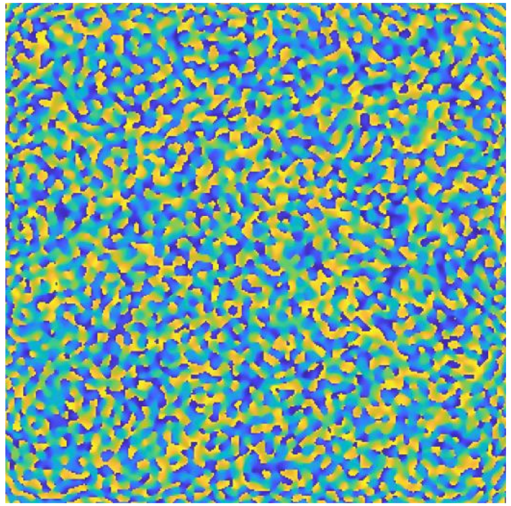

$\angle\, [U_i(u,v;\nu_1) U_i^*(u,v;\nu_2)]$

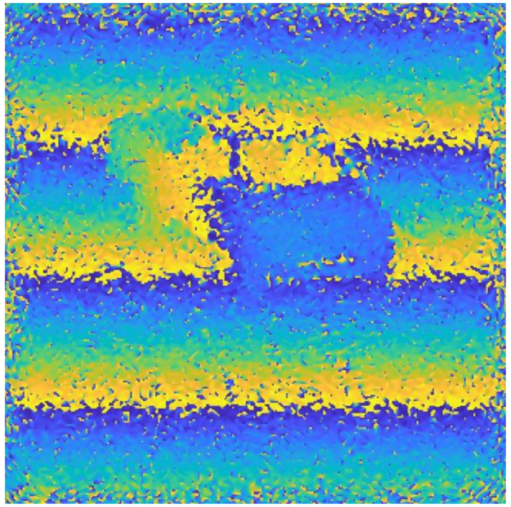

Marron, J. C., et al. "Extended-range digital holographic imaging." *Laser Radar Technology and Applications XV*. Vol. 7684. SPIE, 2010.

Assume that speckle phase is constant over frequency for small bandwidths

$$U_i(u,v;\nu_m) \approx \exp[i4\pi\nu_m z_0/c]\exp[i4\pi\nu_m Z_d(u,v)/c] \times (h(u,v) * \{U_{0,\perp}(u,v)\exp[i4\pi\nu_0 Z_r(u,v)/c]\})$$

- What happens when we Fourier transform $U_i(u,v;\nu)$ over ν_m?

$$\mathcal{F}_{\nu_m}\{U_i(u,v;\nu_m)\} = \mathcal{A}(u,v)\mathcal{F}_{\nu_m}\{\exp\{i4\pi\nu_m[z_0 + Z_d(u,v)]/c\}\}\Big|_{f_{\nu_m}=\frac{2z}{c}}$$

- Phase of $\mathcal{A}(u,v)$ is "**speckle phase**" and is independent of ν_m
- Examine single transverse coordinate (u,v)

The coarse depth phase varies linearly with frequency for each transverse pixel

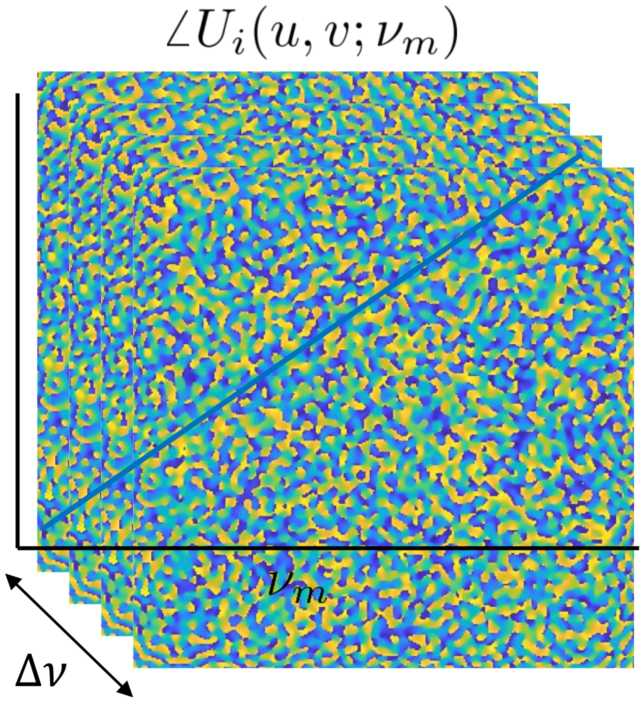

Spoiler alert for later in the talk:
Speckle phase can change with frequency due purely to *diffraction*

Fourier transforming over frequency yields a 3D coherent image

$$\mathcal{F}_{\nu_m}\{U_i(u,v;\nu_m)\} = \mathcal{A}(u,v)\mathcal{F}_{\nu_m}\{\exp\{i4\pi\nu_m[z_0 + Z_d(u,v)]/c\}\}\Big|_{f_{\nu_m}=\frac{2z}{c}}$$

- Use the Fourier shift theorem to write

$$\mathcal{F}_{\nu_m}\{U_i(u,v;\nu_m)\} \propto \mathcal{A}(u,v)\mathcal{F}_{\nu_m}\{B(\nu_m)\} * \delta\{z - [z_0 + Z_d(u,v)]\}$$

- $B(\nu_m)$ is the optical frequency spectrum with width $\Delta\nu$
- $\mathcal{F}_{\nu_m}\{B(\nu_m)\}$ determines range resolution: $c/(2\Delta\nu)$

Fourier transforming over frequency grants access to the object depth profile

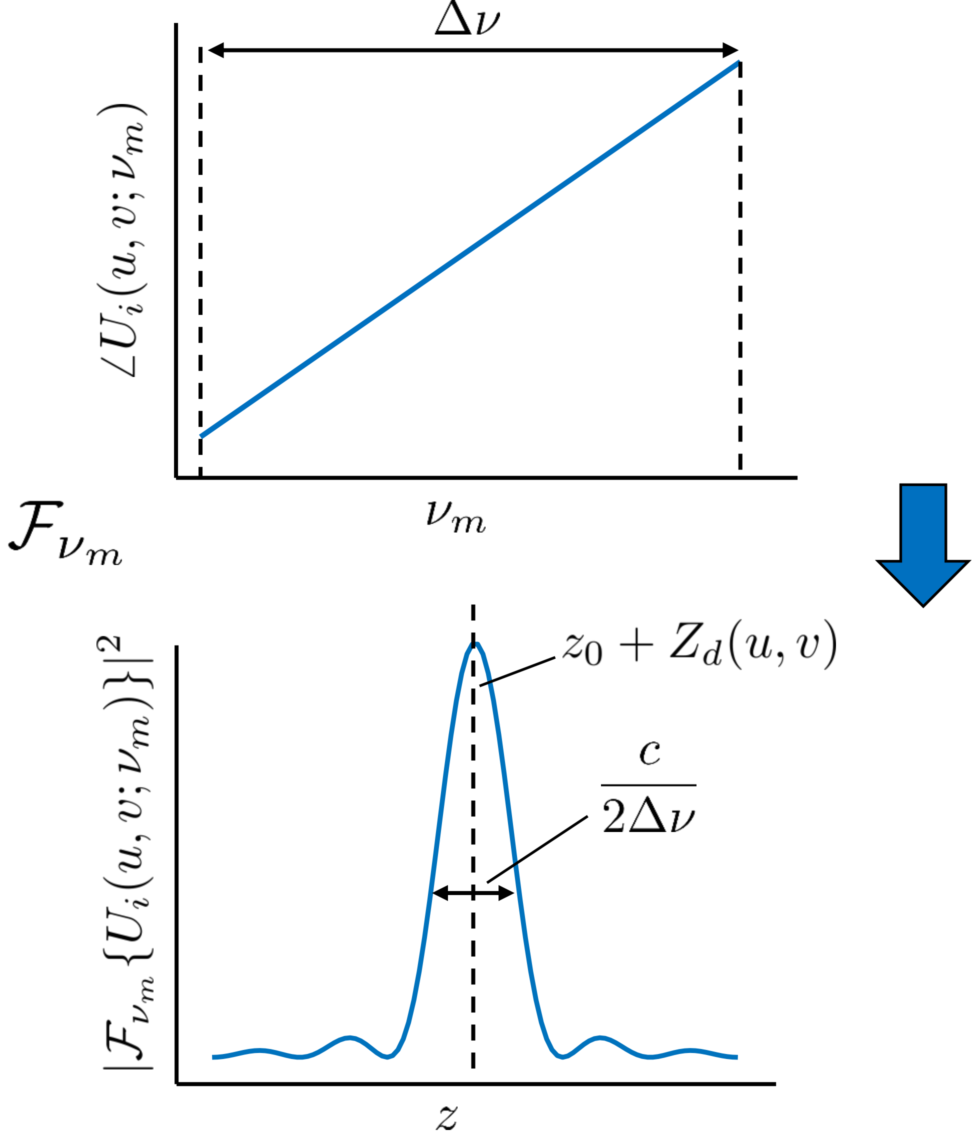

What happens when speckle phase changes pulse to pulse?

- Underlying object reflectance for illumination frequency, ν:

$$A(\xi,\eta)\exp[i\phi(\xi,\eta)]$$

$$\phi(\xi,\eta) = \frac{4\pi\nu}{c}[z_0 + \underline{Z_d(\xi,\eta)} + \underline{Z_r(\xi,\eta)}]$$

$$\phi_r(\xi,\eta) = \frac{4\pi\nu}{c} Z_r(\xi,\eta)$$

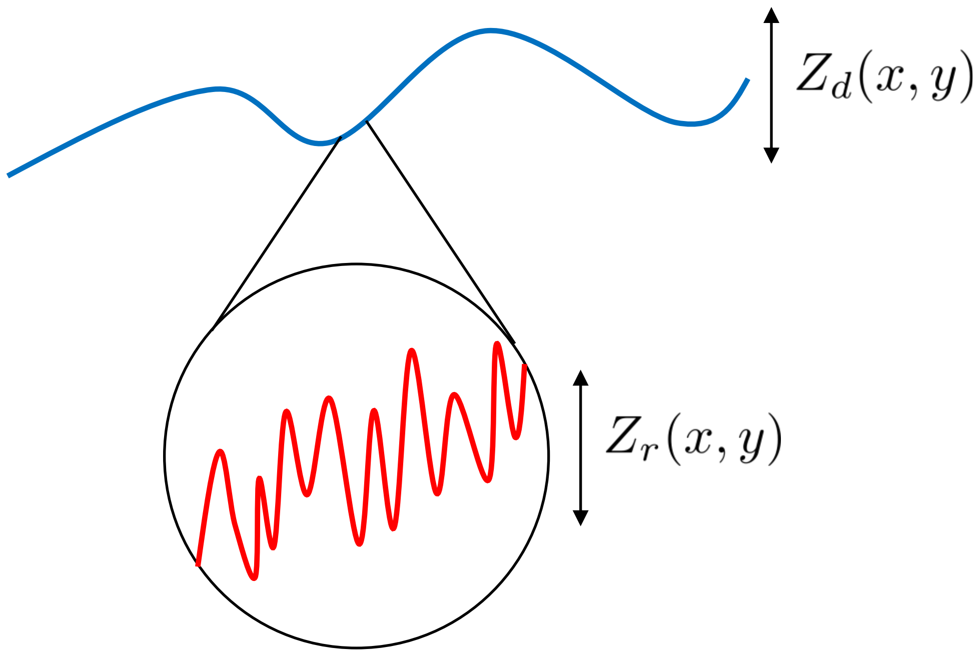

- We are assuming that ϕ_r does not change for small changes in ν, but it can still change when Z_r changes!

Speckle phase in the image plane must have some degree of correlation pulse-to-pulse in order to form a range image

Conventional 3D imaging: what if the surface roughness profile changes over time?

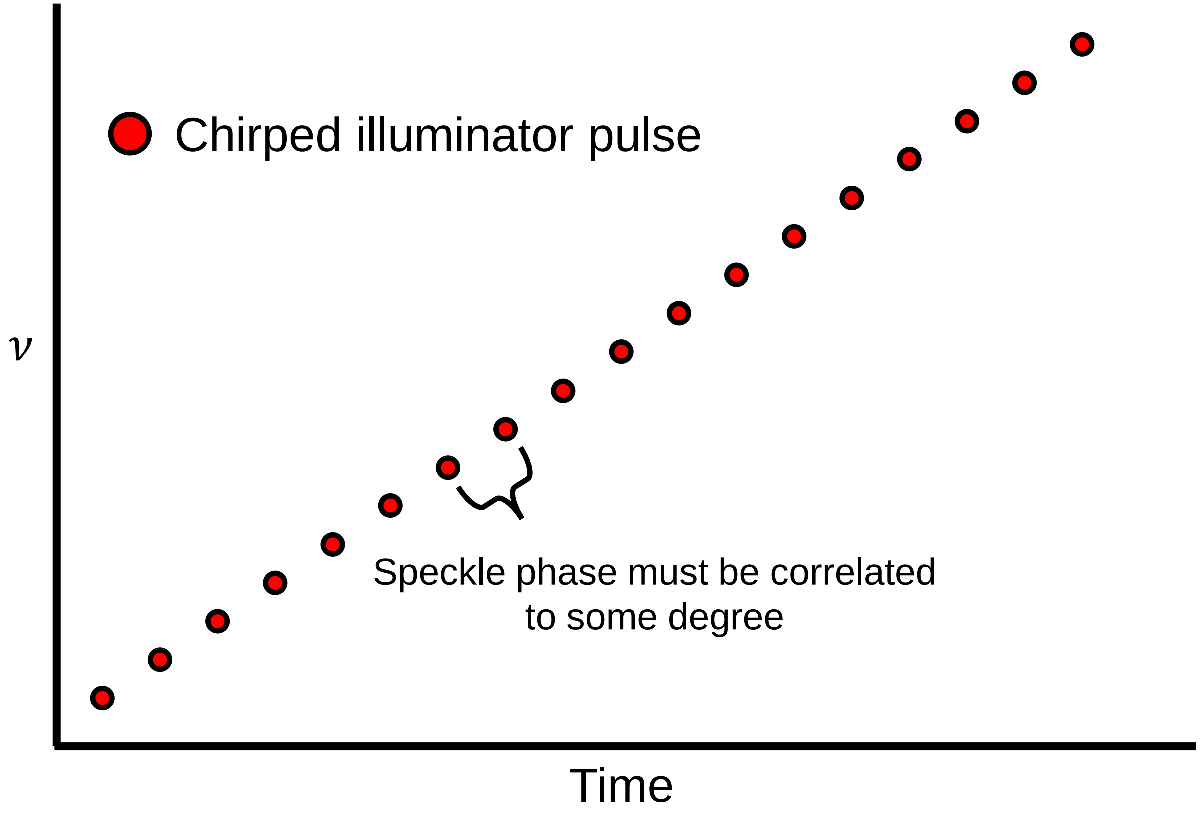

Range images

Common or correlated speckle phase pulse-to-pulse

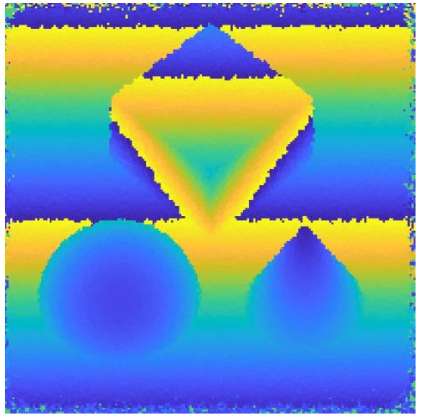

Independent speckle phase pulse-to-pulse

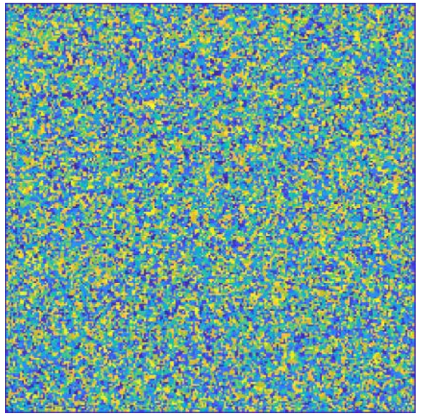

Can occur when object is moving/vibrating over image collection

Adding a second illuminator: Pilot tone

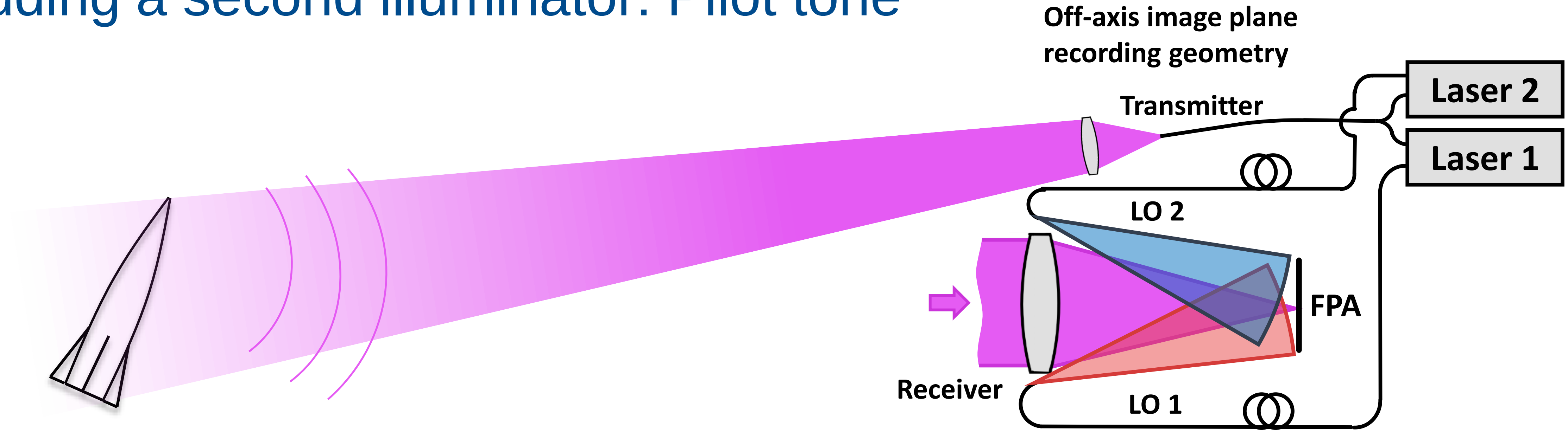

= pilot tone = chirped illuminator = both sources

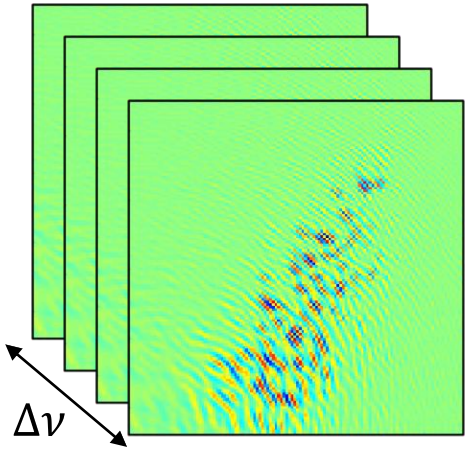

- Flood illuminate distant object with coherent light from **two illuminators**
- Interfere images of object with off-axis reference beams resulting in a **multiplexed hologram**
- Repeat for many frequencies in a narrow bandwidth
- Perform Fourier transform over optical frequency to generate 3D image

Krause, B. (2017). U.S. Patent No. 9,581,967. Washington, DC: U.S. Patent and Trademark Office.
Krause, B. W., Tiemann, B. G., & Gatt, P. (2012). Motion compensated frequency modulated continuous wave 3D coherent imaging ladar with scannerless architecture. *Applied optics*, *51*(36), 8745-8761.

Addition of Brian Krause’s pilot tone enables motion compensation

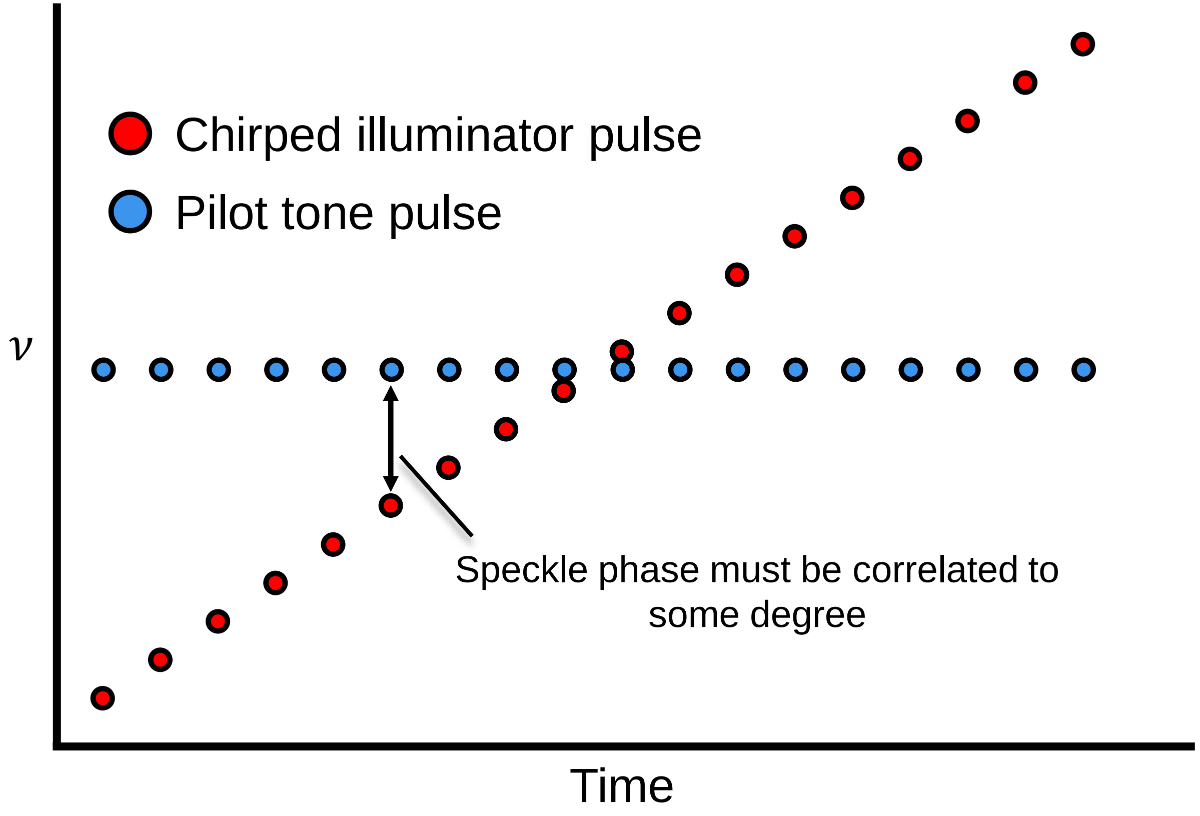

Range images

Independent speckle phase pulse-to-pulse
Pilot tone OFF

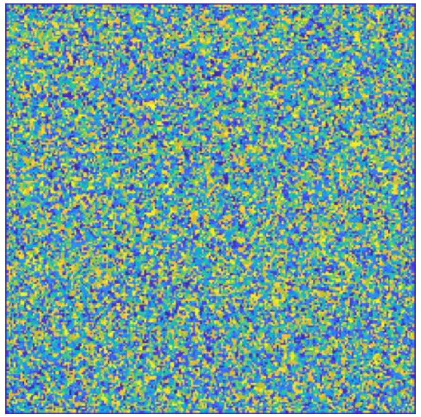

Independent speckle phase pulse-to-pulse
Pilot tone ON

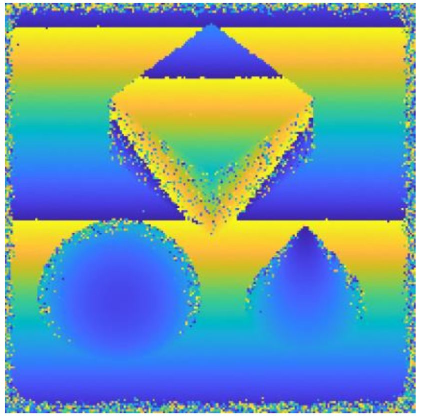

Robust to object motion/vibration

Krause, B. (2017). U.S. Patent No. 9,581,967. Washington, DC: U.S. Patent and Trademark Office.
Krause, B. W., Tiemann, B. G., & Gatt, P. (2012). Motion compensated frequency modulated continuous wave 3D coherent imaging ladar with scannerless architecture. *Applied optics*, *51*(36), 8745-8761.

Processing for multiplexed holograms

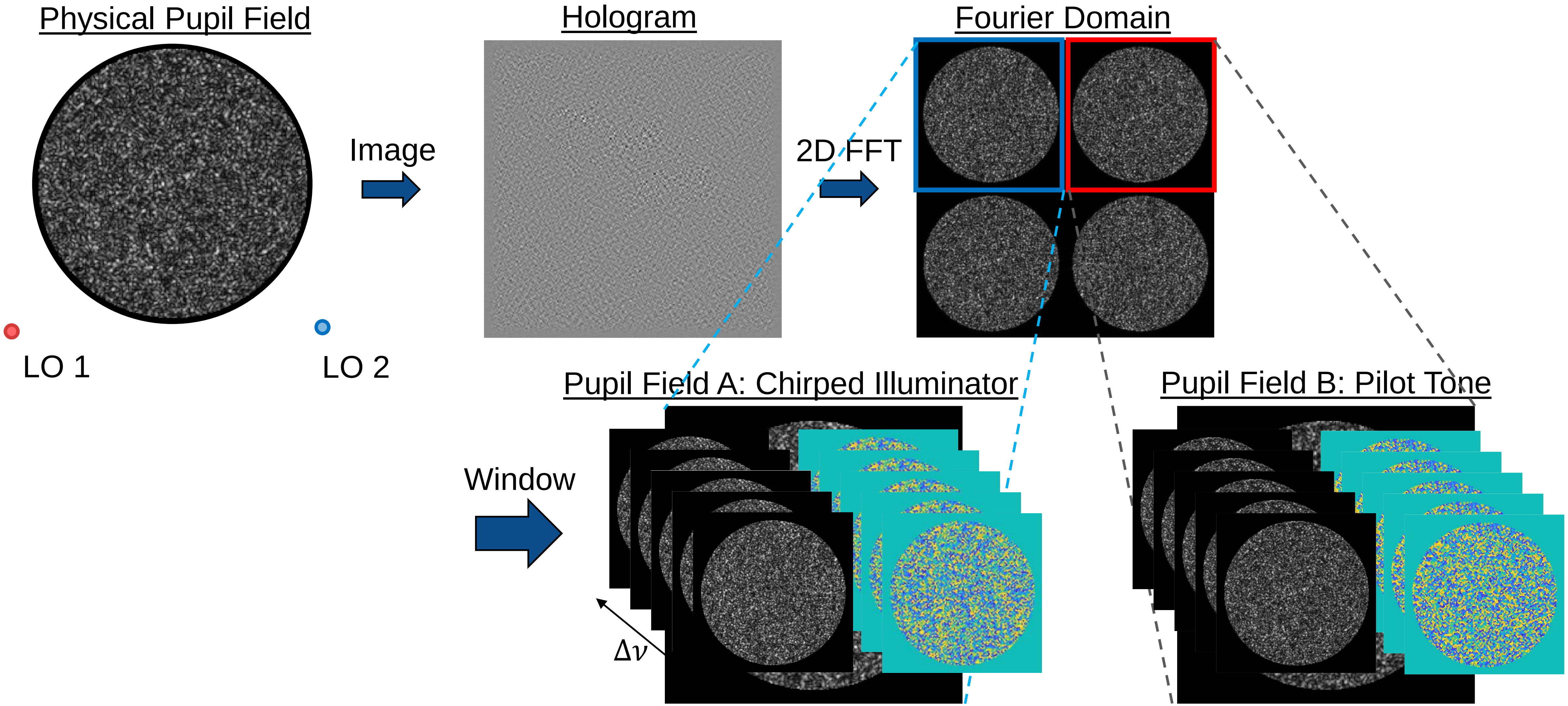

Conjugate product images

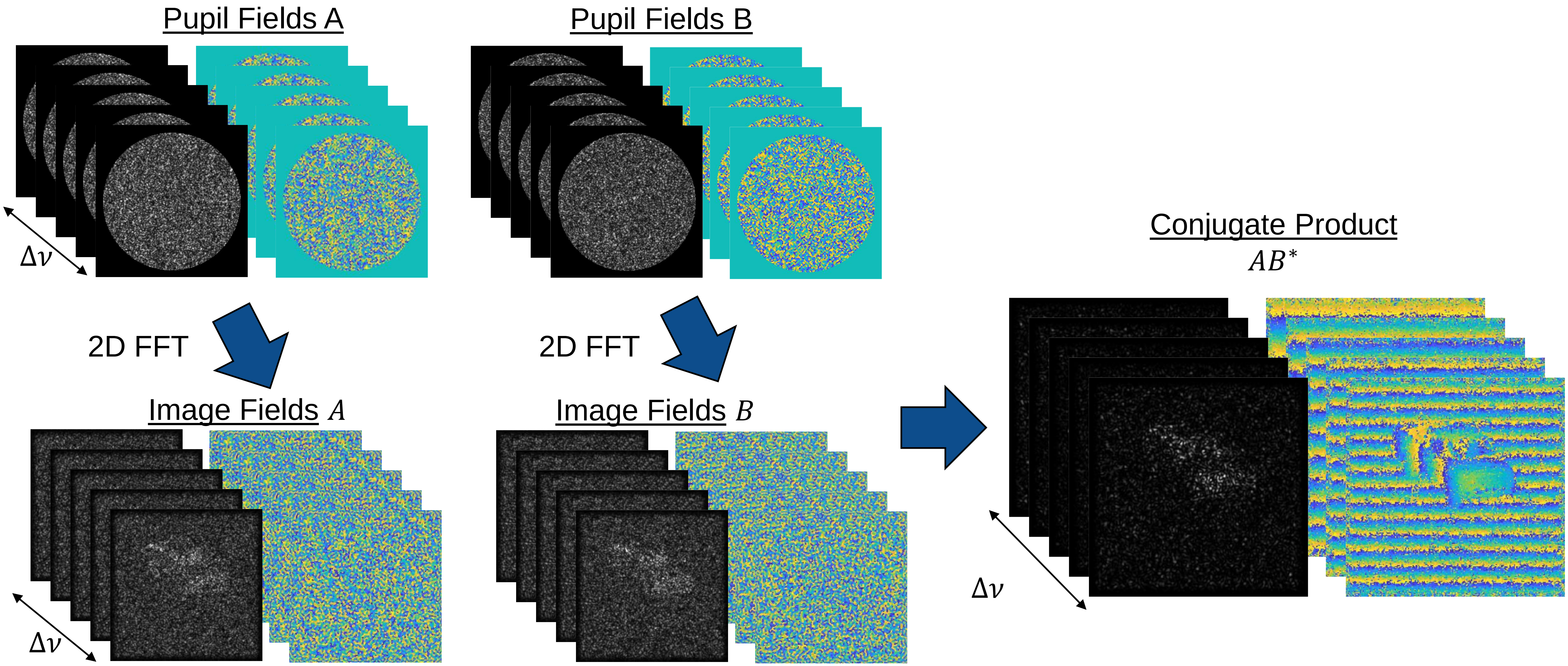

3D image formation with a pilot tone

Conjugate Product AB^*

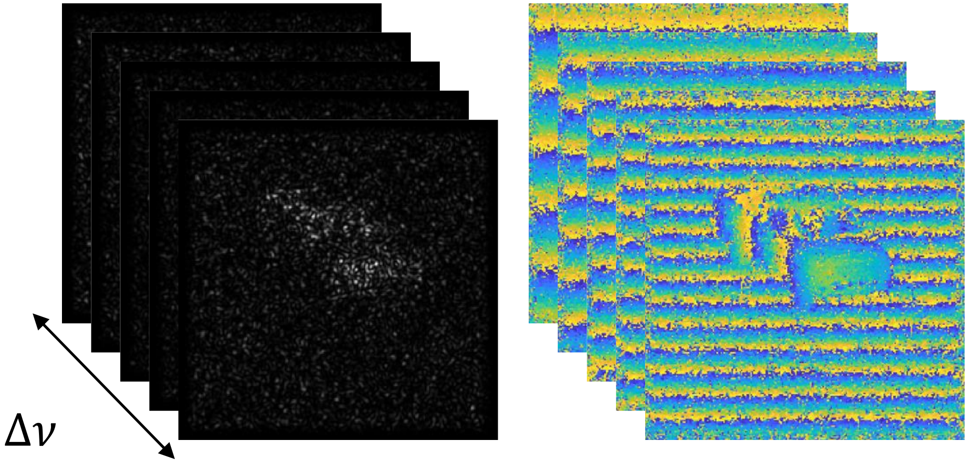

1D FFT

3D Irradiance Cloud

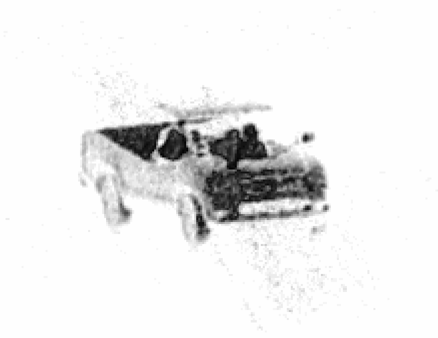

2D Frequency-Averaged Image

Range Image

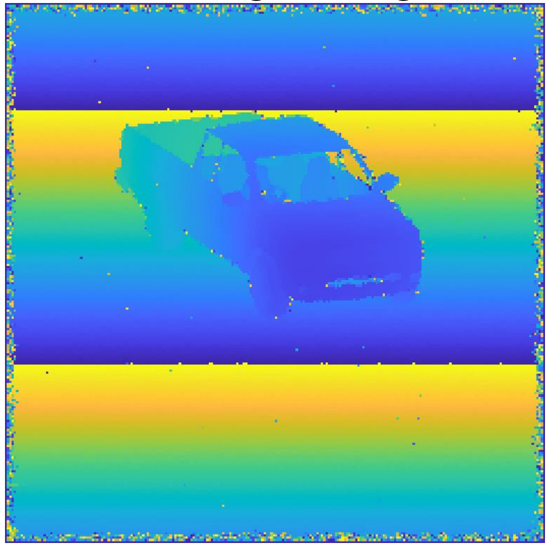

- Range image found by location of max irradiance at each x, y
- Speckle averaging can occur

Speckle averaging occurs when speckle phase is uncorrelated pulse-pair to pulse-pair

How does one form a 3D image via conjugate product images?

- Take **conjugate product** of images with in a pulse pair

- Remaining phase shows optical path difference between the chirped illuminator and pilot tone

$$E_n(u,v;\nu_n-\nu_p) = U_n(u,v;\nu_n)U^*_{n,pilot}(u,v;\nu_p)$$

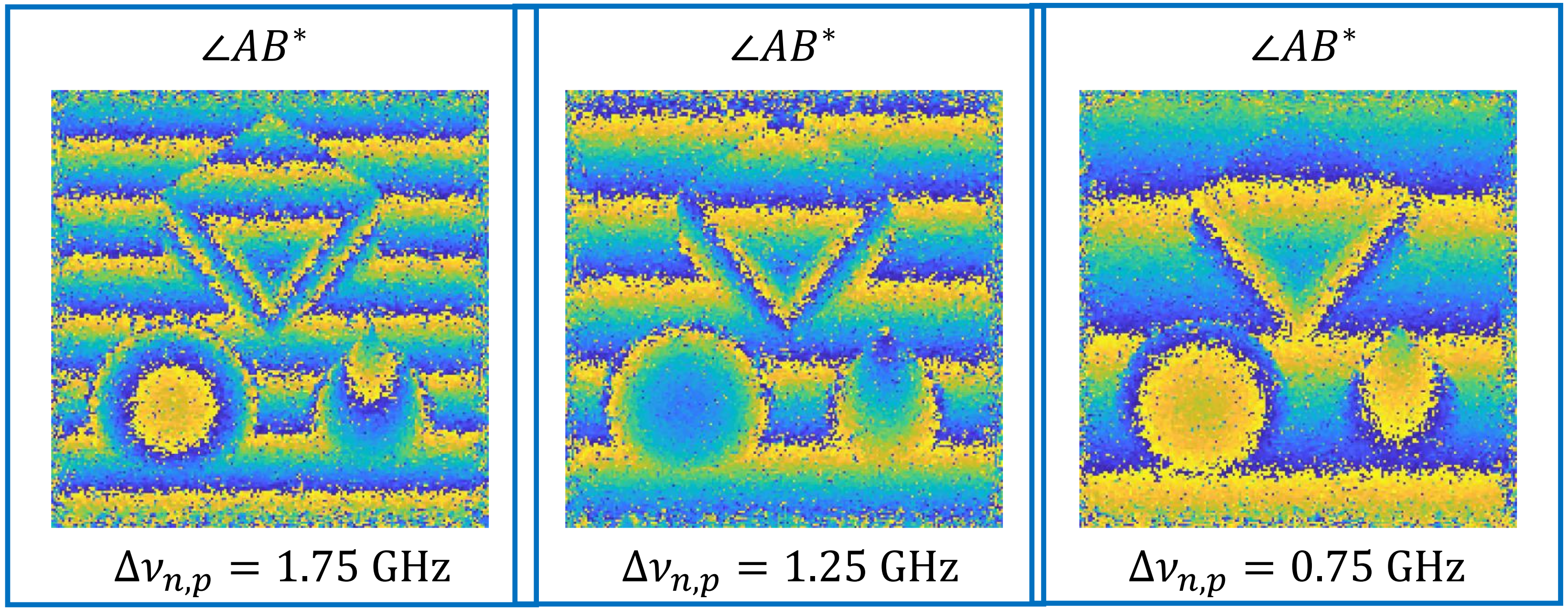

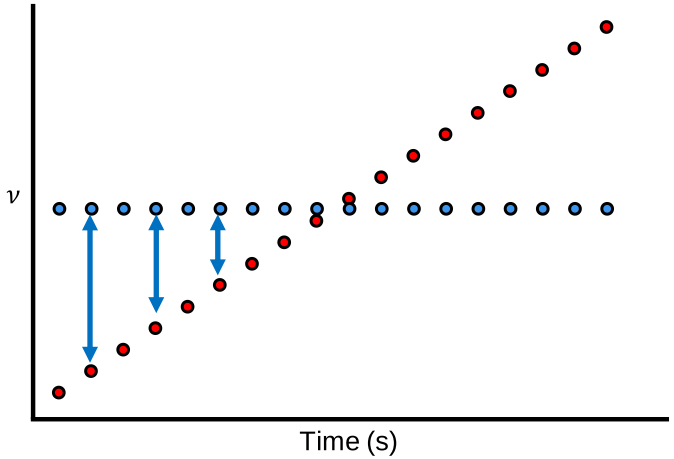

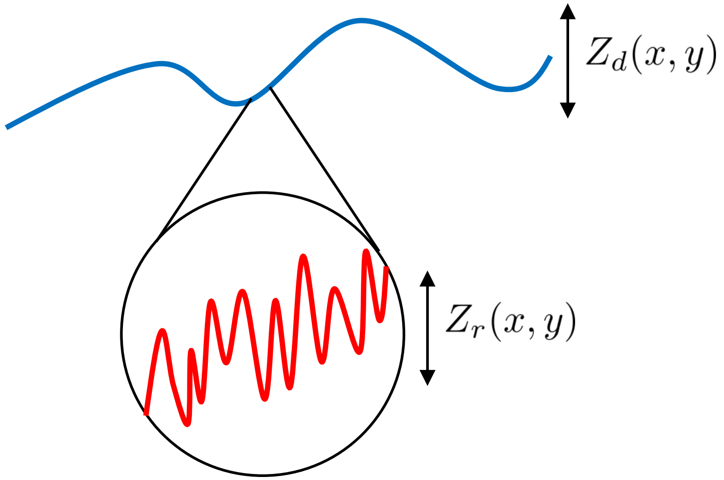

With pilot-tone 3D imaging, range chatter can appear for sloped object facets

Range image formed w/o pilot tone

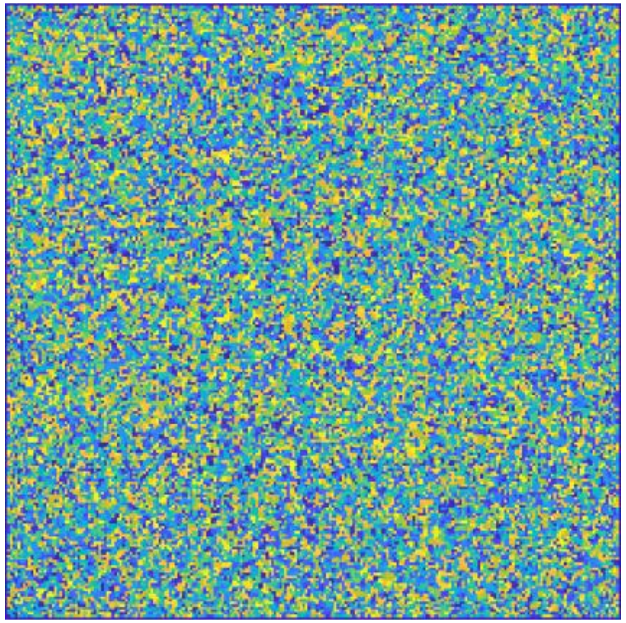

Range image formed w/ pilot tone

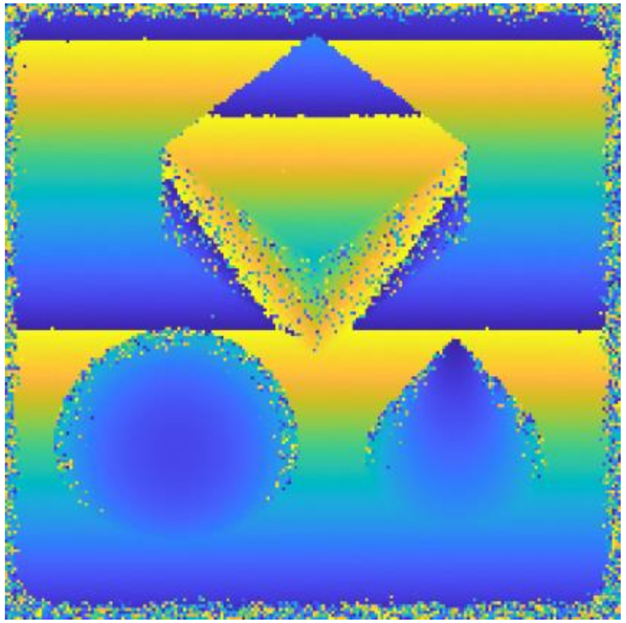

Spoiler confirmed:
Range chatter is due to speckle phase changing with frequency due purely to *diffraction*

Range chatter can appear over sloped object facets for even in the case of infinite SNR!

Speckle shifting for sloped objects: Changing tilt

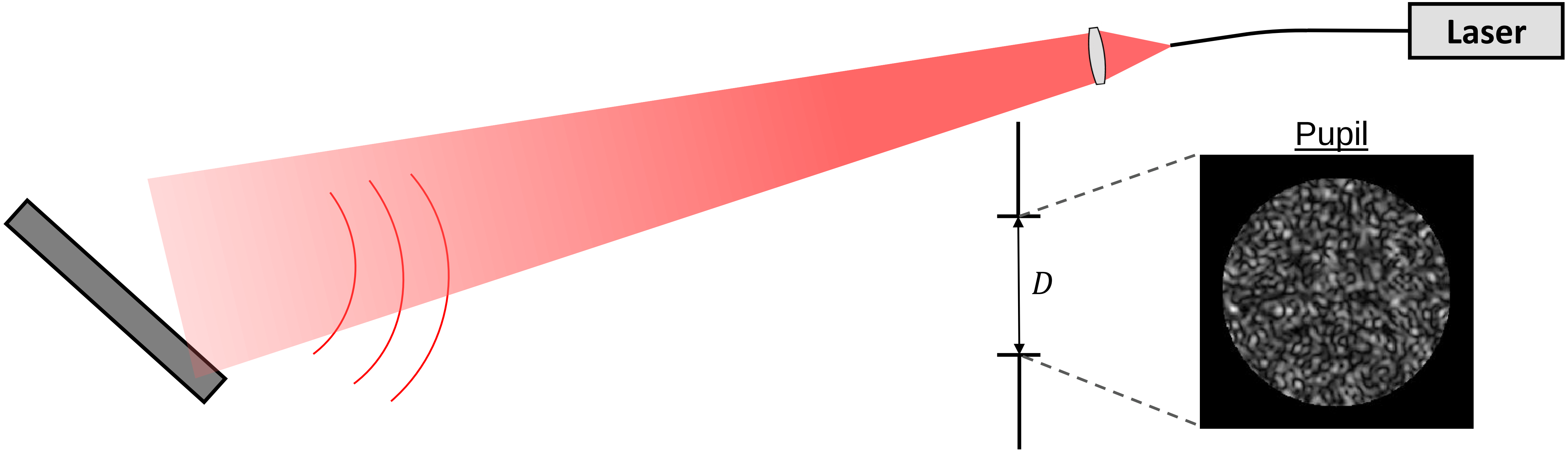

Speckle pattern in pupil shifts with object tilt

Speckle shifting for sloped objects: Changing frequency causes speckle decorrelation

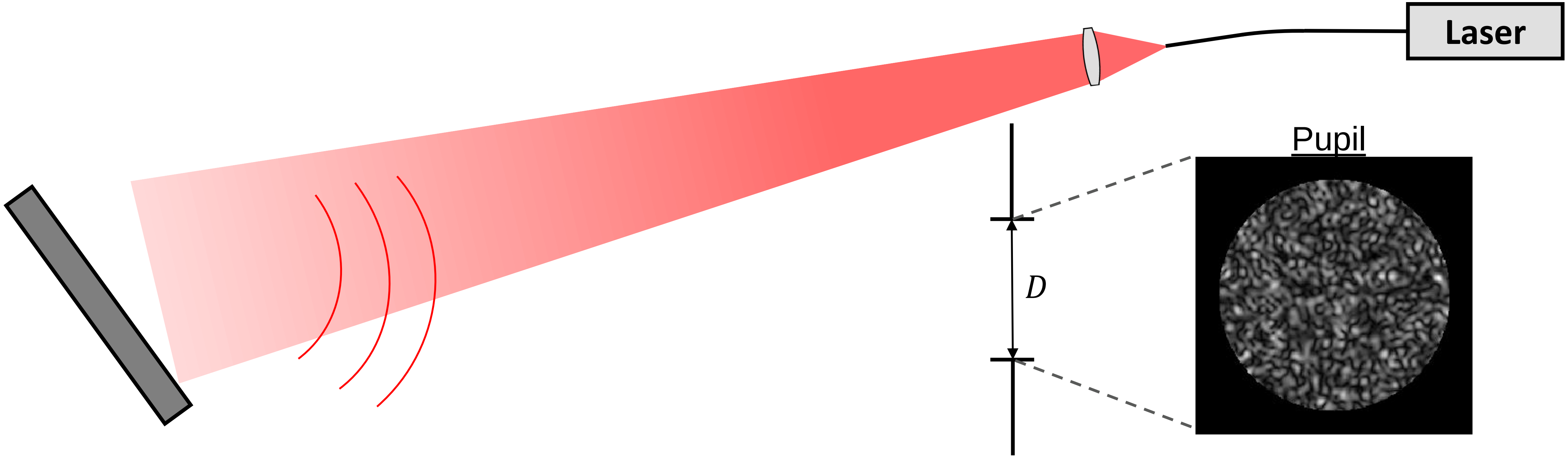

Speckle pattern in pupil shifts with changing frequency

Defining the object phase difference for two illumination frequencies

- Define a frequency difference within a pair of frequencies ν_1 and ν_2, $|\nu_1 - \nu_2| = \boldsymbol{\Delta\nu_{1,2}}$

$$A(\xi,\eta)\exp[i\phi(\xi,\eta)]$$

$$\phi(\xi,\eta) = \frac{4\pi\nu}{c}[z_0 + Z_d(\xi,\eta) + Z_r(\xi,\eta)]$$

- Change in phase, $\Delta\phi(x,y)$ between two frequencies is

$$\Delta\phi(\xi,\eta) = \frac{4\pi}{c}[\Delta\nu_{1,2}z_0 + \Delta\nu_{1,2}Z_d(\xi,\eta) + \Delta\nu_{1,2}Z_r(\xi,\eta)]$$

$$\Delta\phi(\xi,\eta) = \frac{4\pi}{c}\Delta\nu_{1,2}Z_d(\xi,\eta)$$

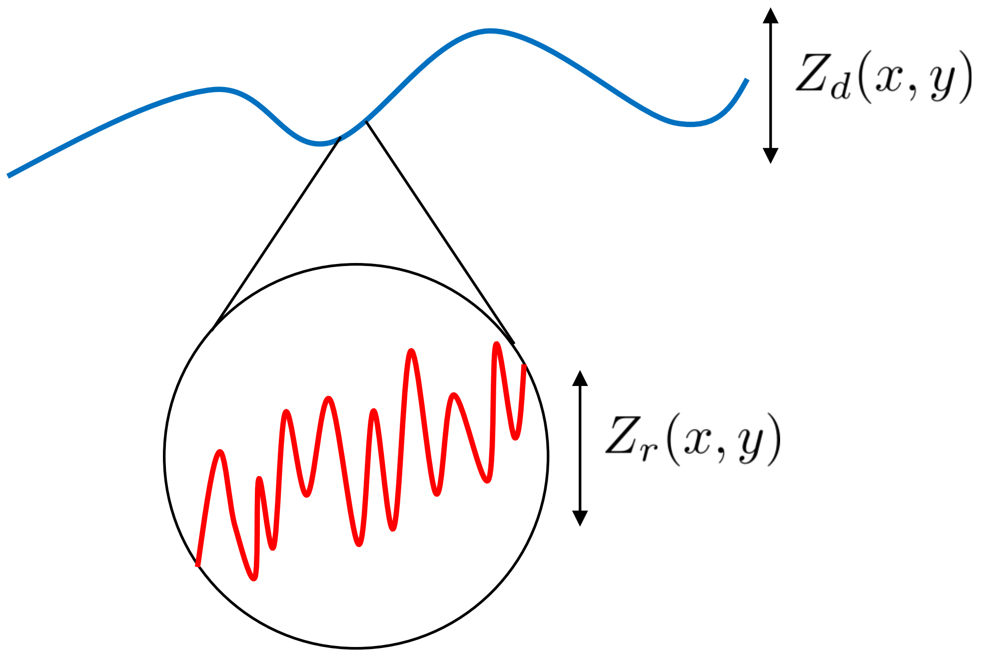

Speckle decorrelation in terms of the slope bandwidth product (SBP)

- Assume $Z_d(x, y) = \alpha x$, a linearly sloped object. Then the $\Delta\phi(x, y)$ yields speckle shift of Δx via **Fourier shift theorem**

$$\frac{4\pi}{c}\Delta\nu_{1,2} Z_d(\xi,\eta) = \frac{4\pi}{c}\Delta\nu_{1,2}\alpha\xi = 2\pi\Delta x f_\xi\Big|_{f_\xi=\xi/(\lambda_0 z_0)} = \frac{2\pi\Delta x\xi}{\lambda_0 z_0}$$

- Taking $\lambda_0 \approx c/\nu_0$

$$\text{SBP} = \boxed{\alpha\frac{\Delta\nu_{1,2}}{\nu_0} = \frac{\Delta x}{2z_0}}$$

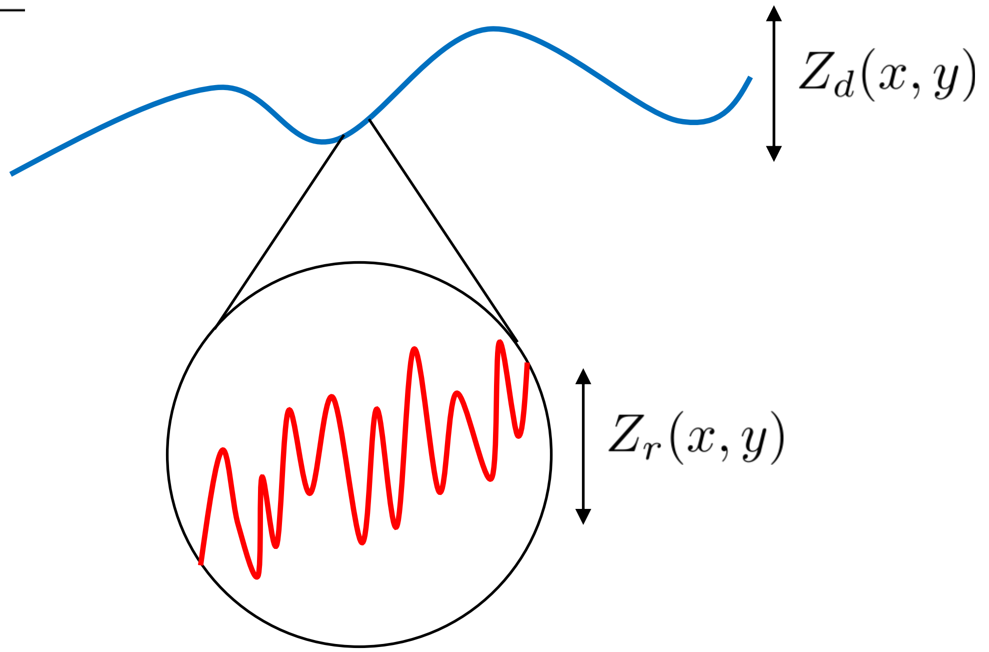

Banet, M. T., & Fienup, J. R. (2023). Speckle decorrelation effects on motion-compensated, multi-wavelength 3D digital holography: theory and simulations. Optical Engineering, 62(7), 073103-073103.

Independent speckle phase pulse-pair to pulse-pair: Conventional 3D imaging

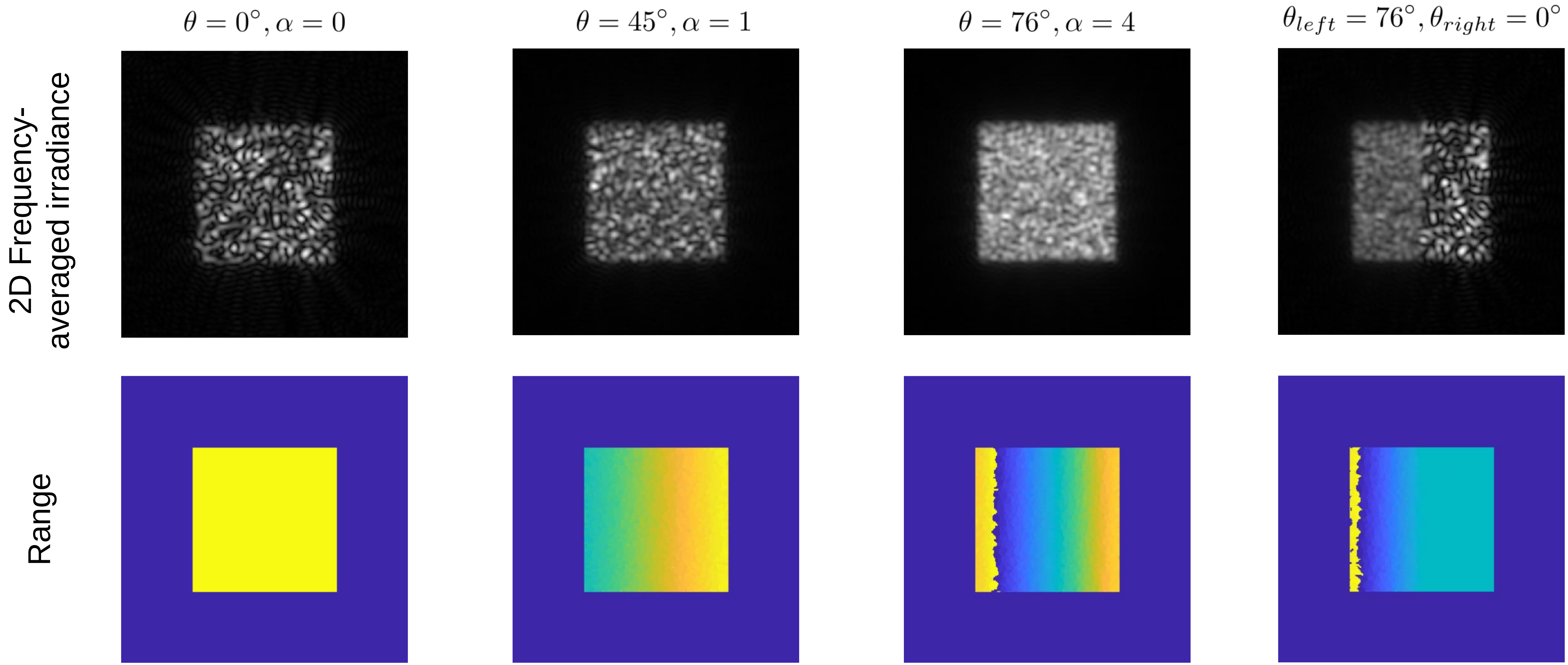

Common or correlated speckle phase pulse-to-pulse: Pilot-tone 3D imaging

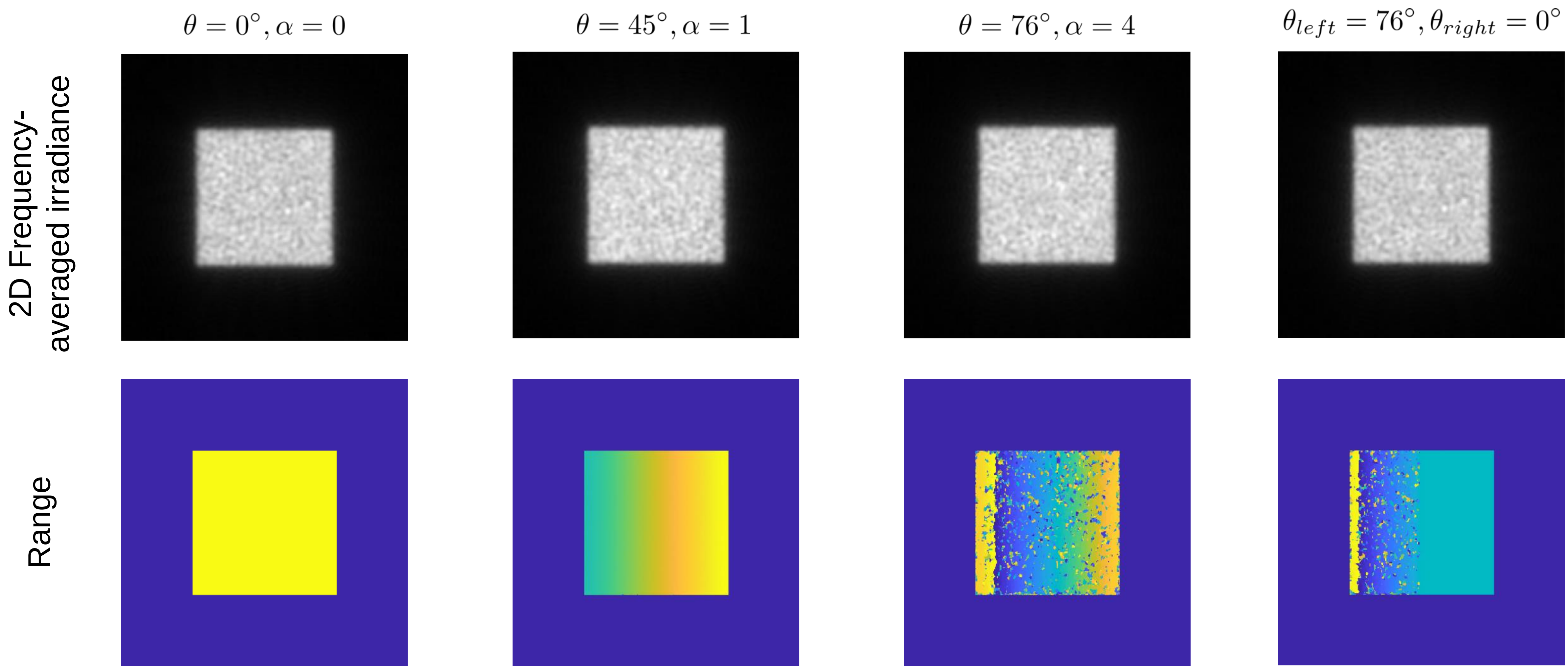

How does changing wavelength change speckle?

- Speckle evolves with changes in wavelength via two mechanisms:†
  1. Changes due to the Fresnel **diffraction** integral as a function of wavelength
  2. Interaction between the variable wavelength and the **surface microstructure**

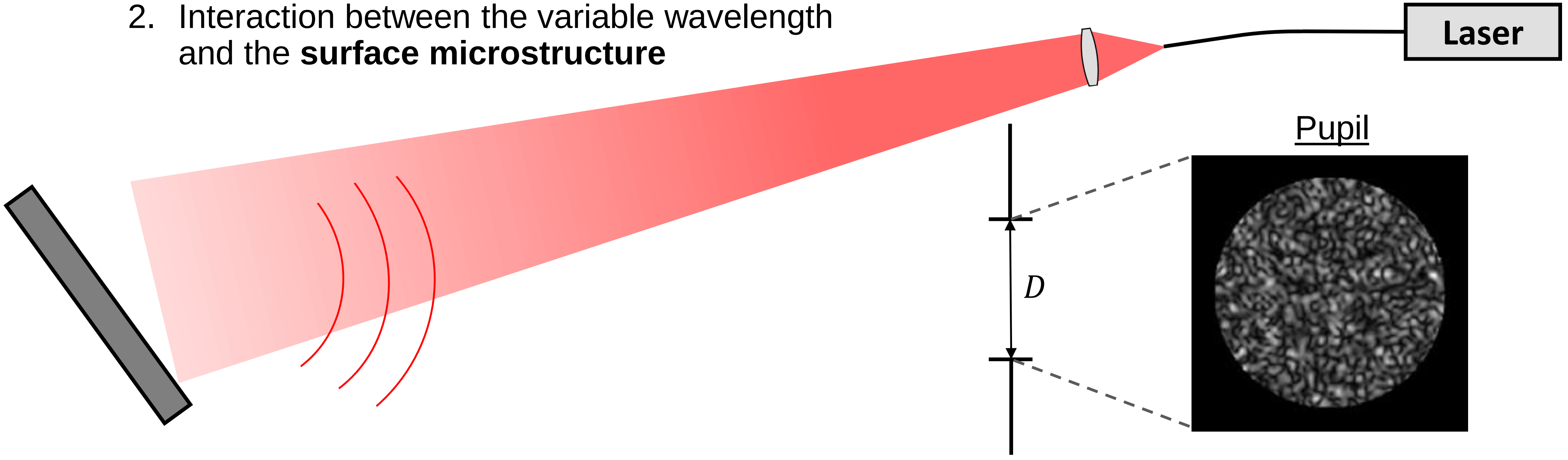

† Goodman, Joseph W., Speckle Phenomena in Optics: Theory and Applications, 2nd ed., SPIE Press, Bellingham, Washington, United States (2020).

What about changes in wavelength?

- Speckle evolves with changes in wavelength via two mechanisms:†
  1. Changes due to the Fresnel **diffraction** integral as a function of wavelength
  2. Interaction between the variable wavelength and the **surface microstructure**

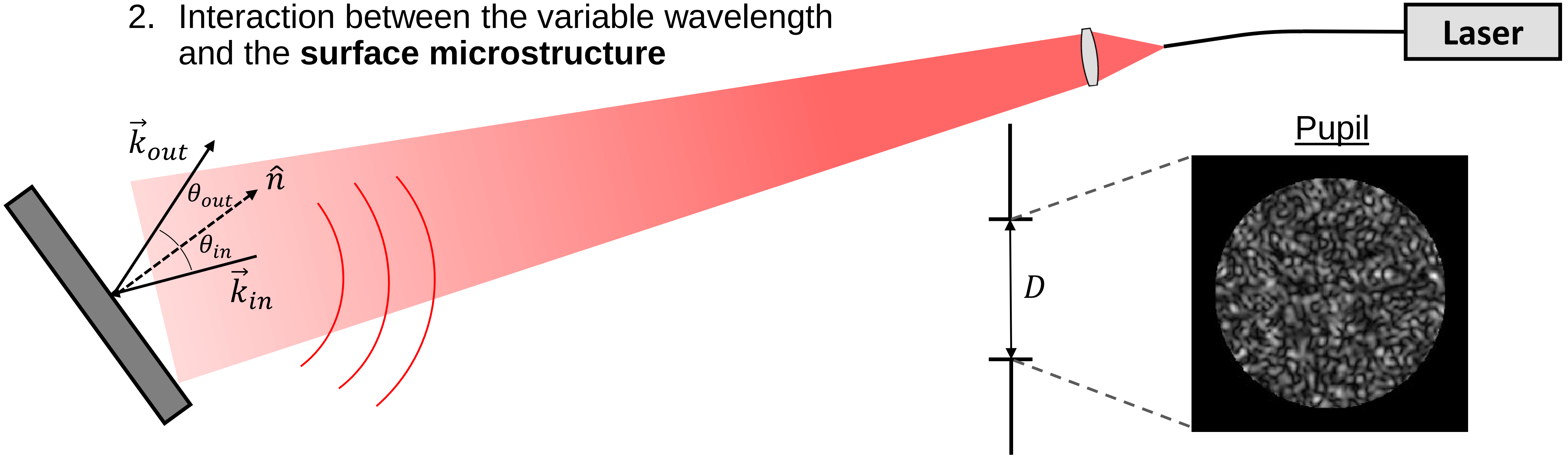

† Goodman, Joseph W., Speckle Phenomena in Optics: Theory and Applications, 2nd ed., SPIE Press, Bellingham, Washington, United States (2020).

Speckles contracting/expanding for a sloped object (small slope, large bandwidth)

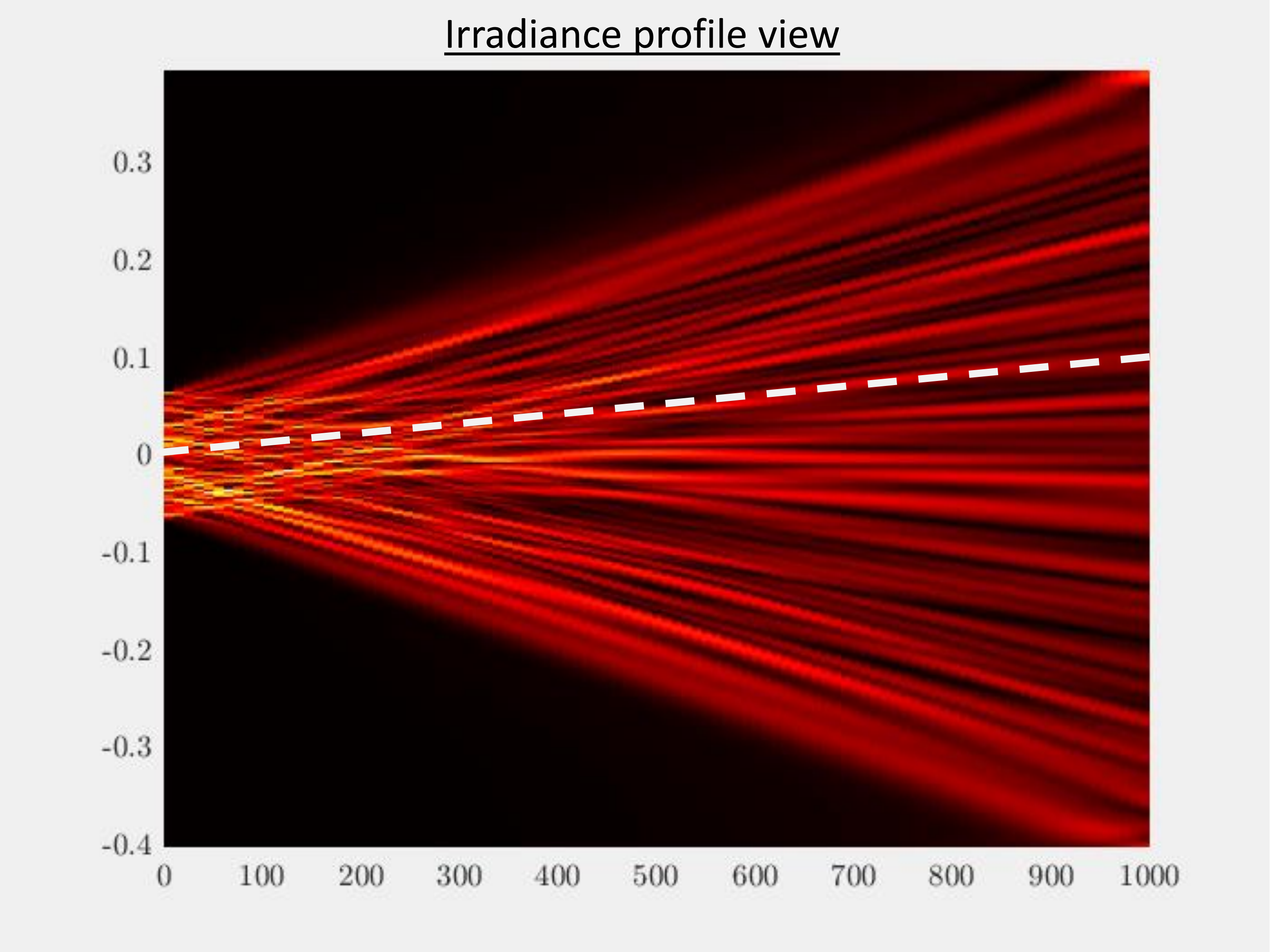

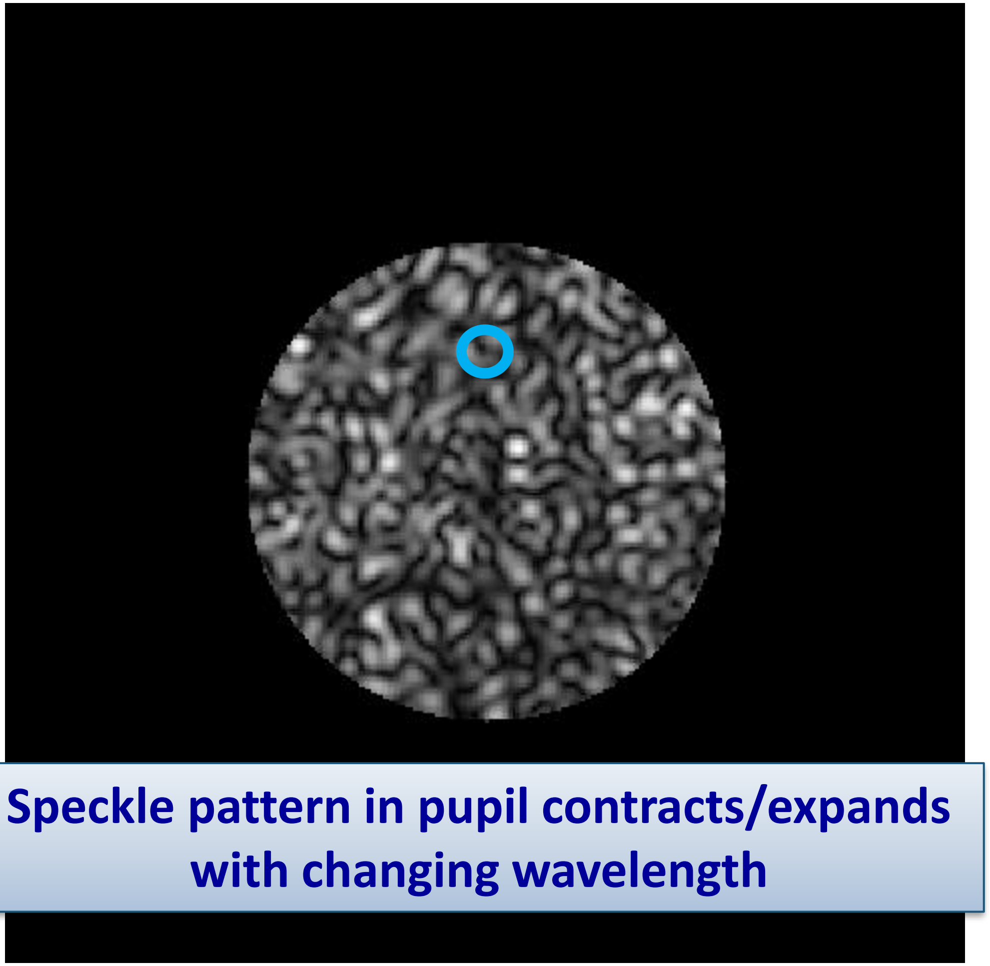

Speckle pattern in pupil contracts/expands with changing wavelength

Speckles translating for a sloped object (large slope, small bandwidth)

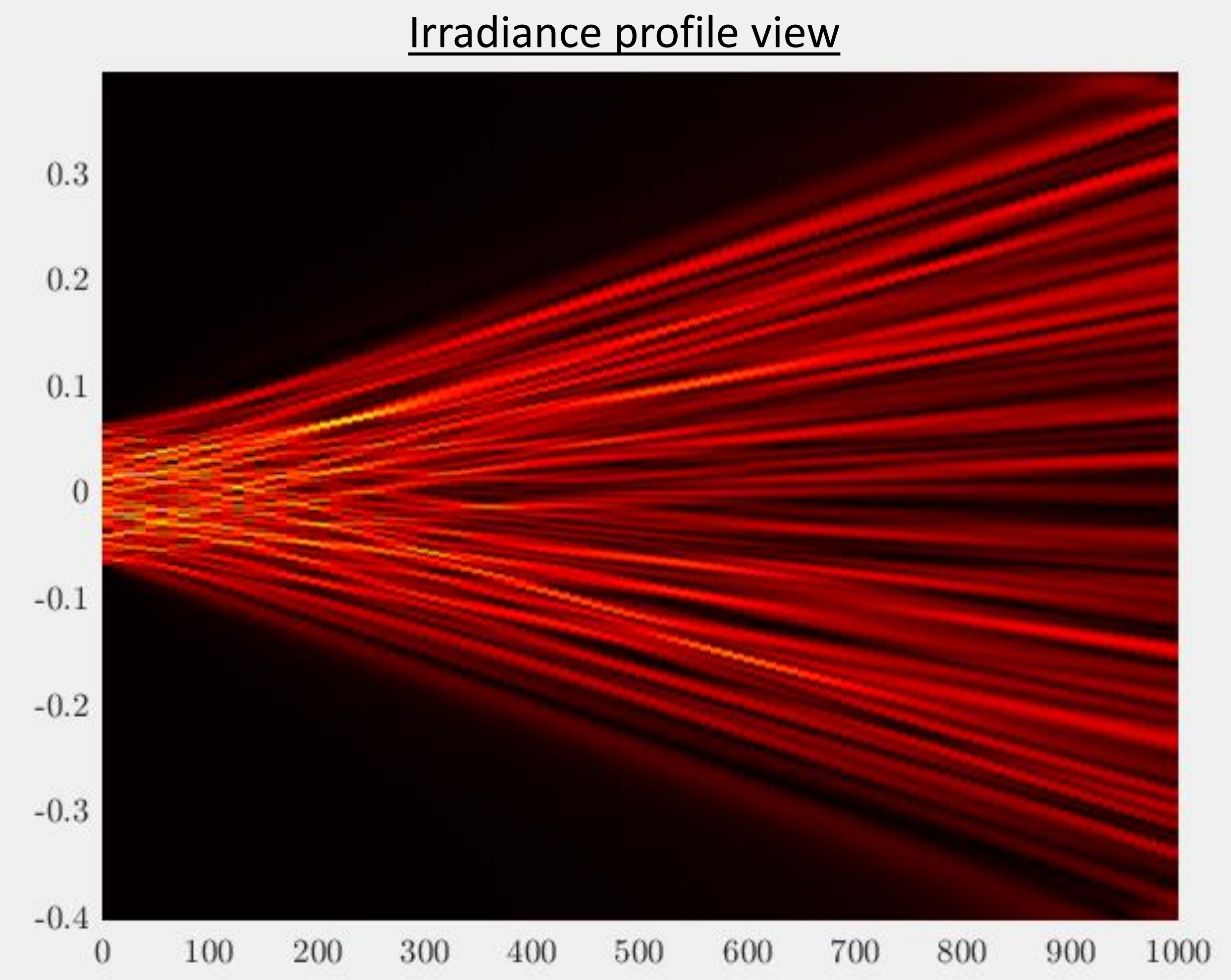

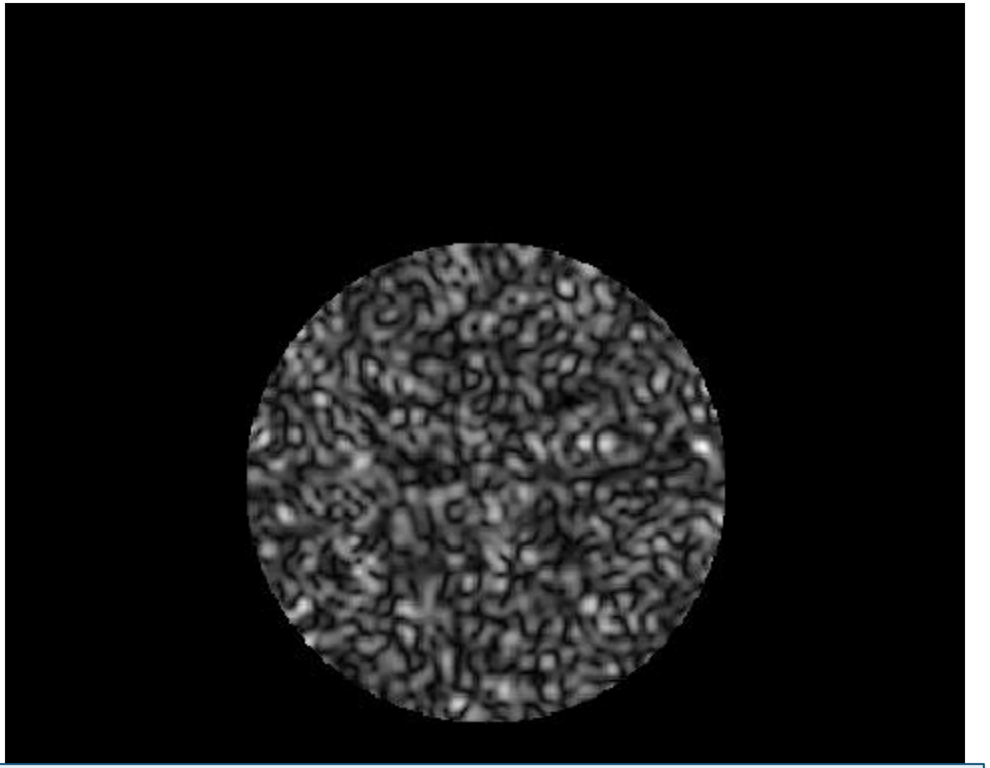

Speckle pattern in pupil translates with changing wavelength

How can we alleviate range chatter?

Range image formed w/o pilot tone

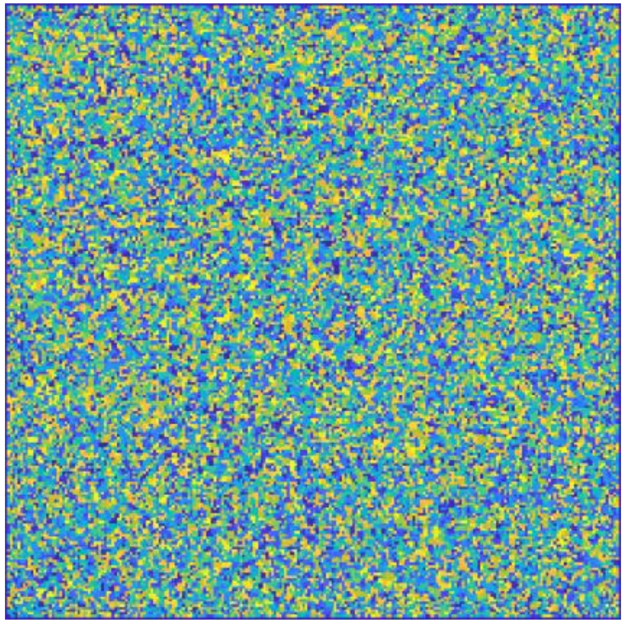

Range image formed w/ pilot tone

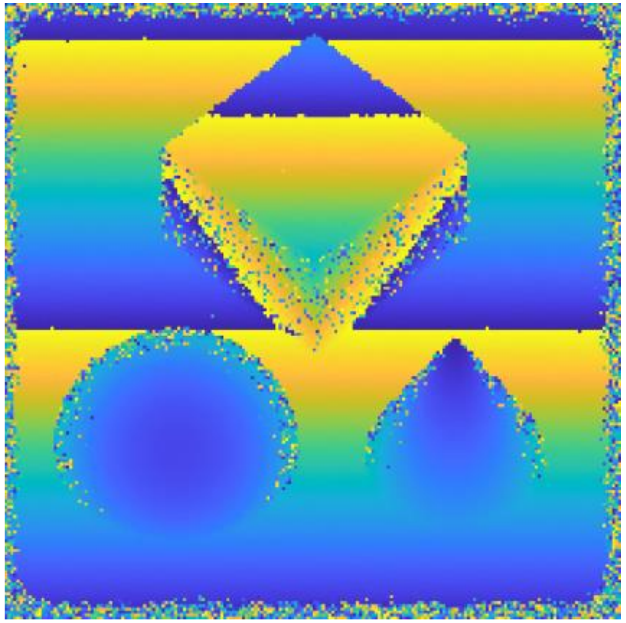

Spoiler confirmed:
Range chatter is due to speckle phase changing with frequency due purely to *diffraction*

Range chatter can appear over sloped object facets even in the case of infinite SNR!

Dual tone 3D imaging

Speckle phase is highly correlated within pulse pairs

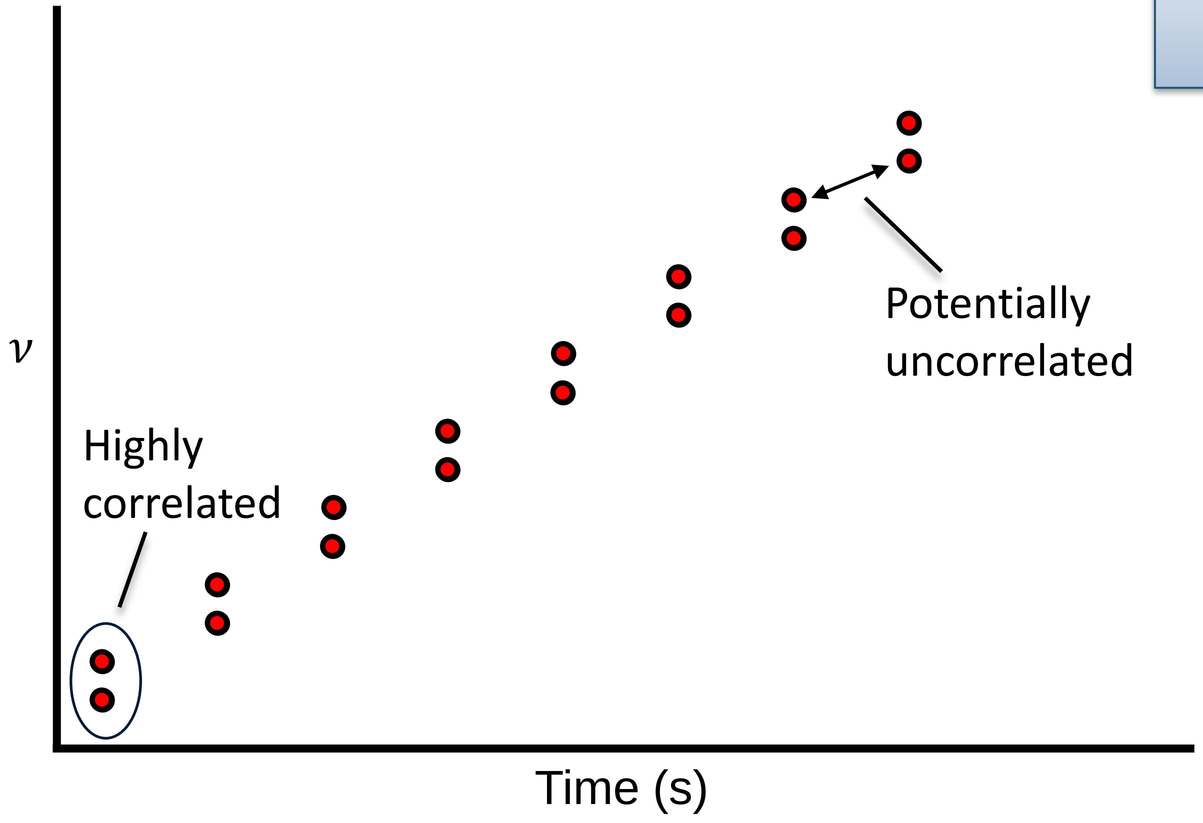

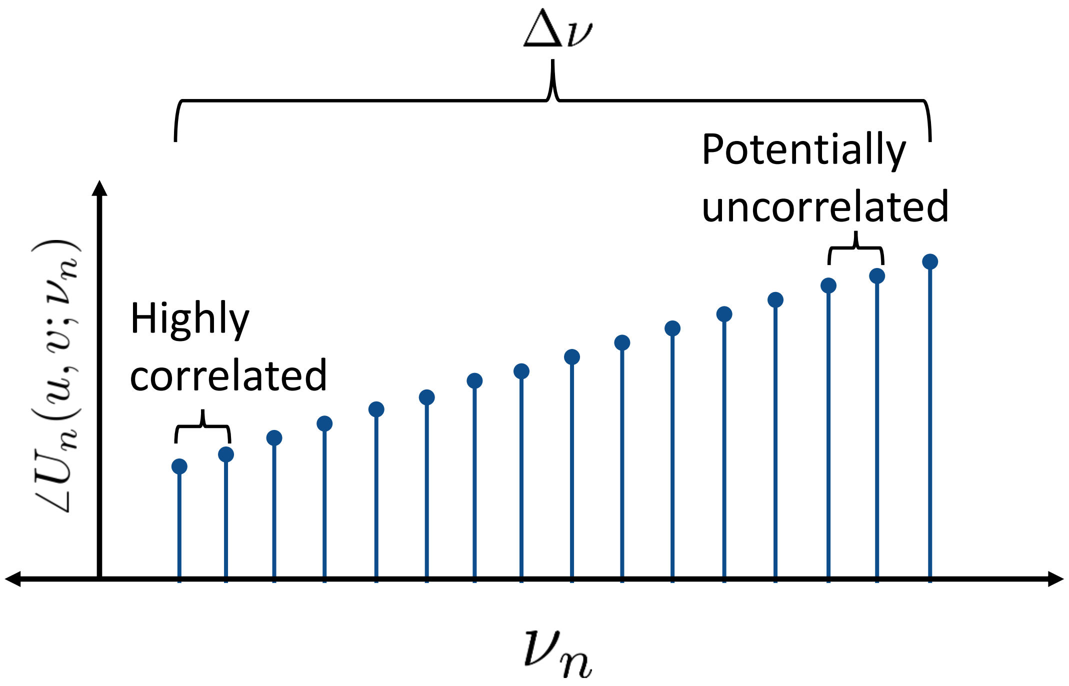

Total number of samples in optical frequency domain, $S = 16$

Stairstep 3D imaging: pulse configuration

Redundant frequency measurements sample frequency-difference space

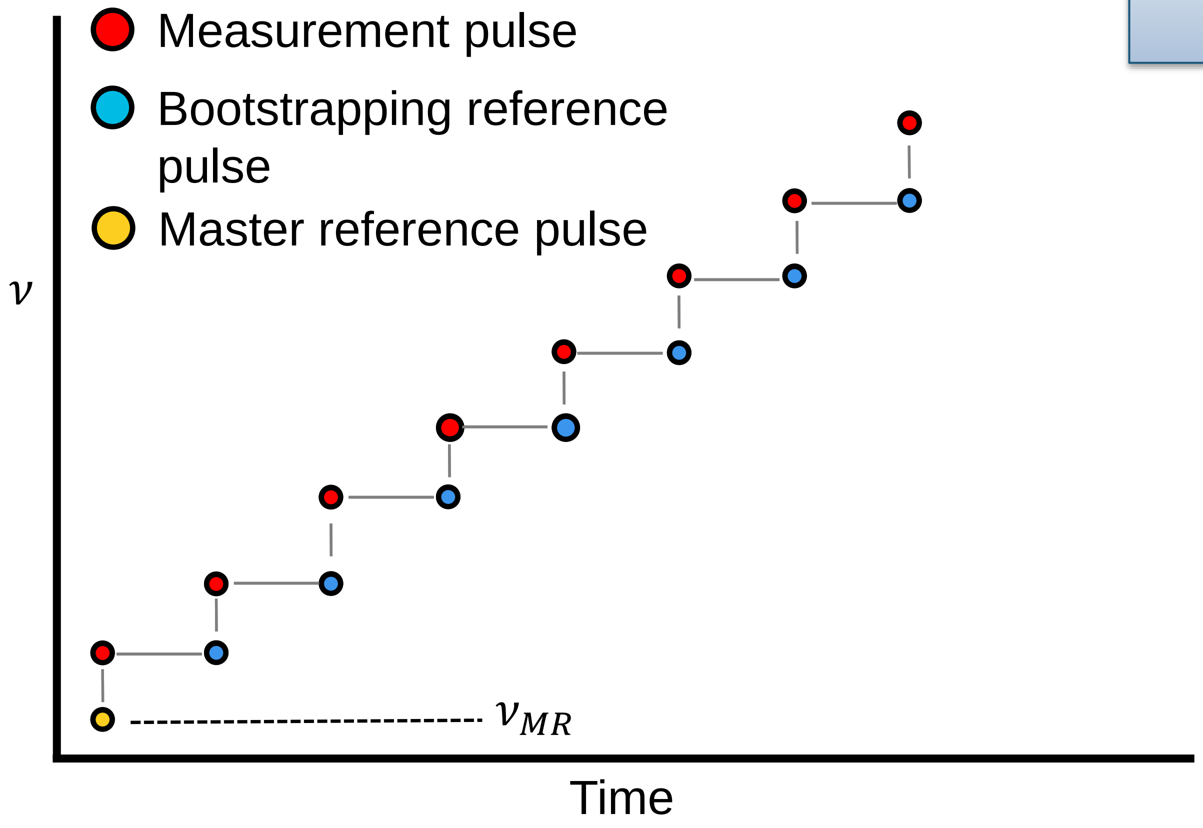

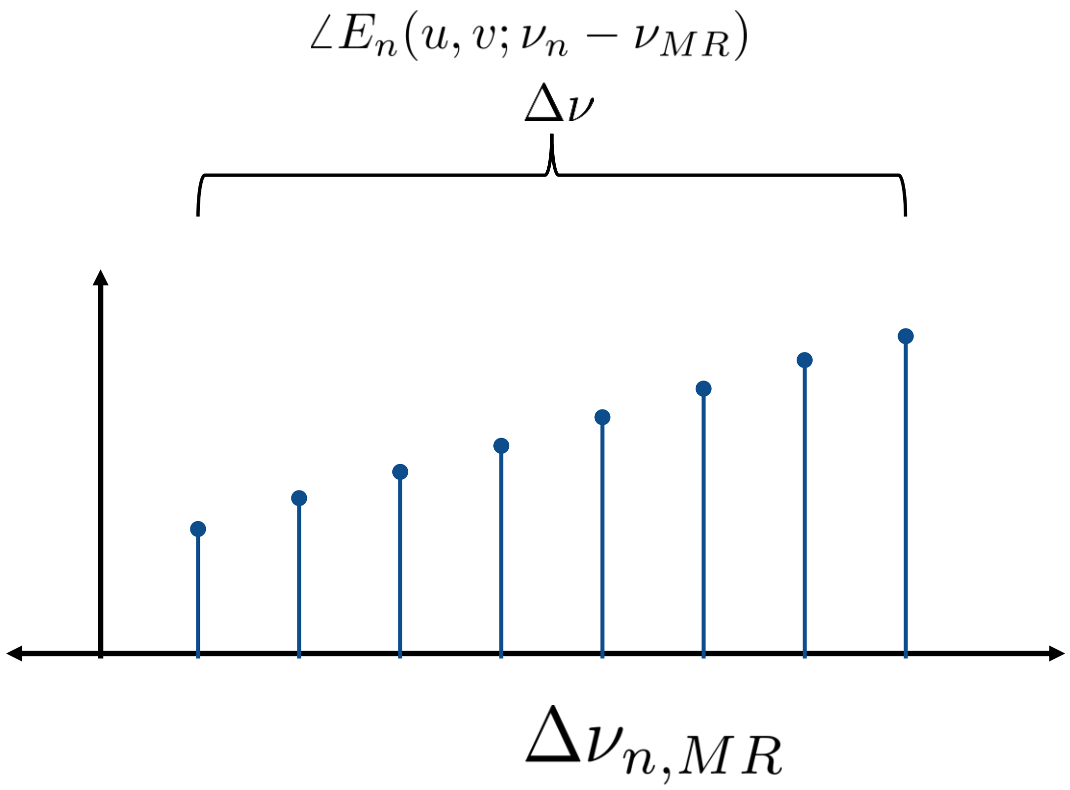

Stairstep 3D imaging: frequency difference images

$$U(u,v;\nu) \approx A(u,v)\exp(i4\pi\nu z_0/c)\,\underline{\exp[i4\pi\nu Z_d(u,v)/c]\exp[i\phi_r(u,v)]}$$

$$\angle E_{1,0} = \angle U_1 U_0^*$$

$$\angle E_{3,0} = \angle U_3 U_2^* U_1 U_0^*$$

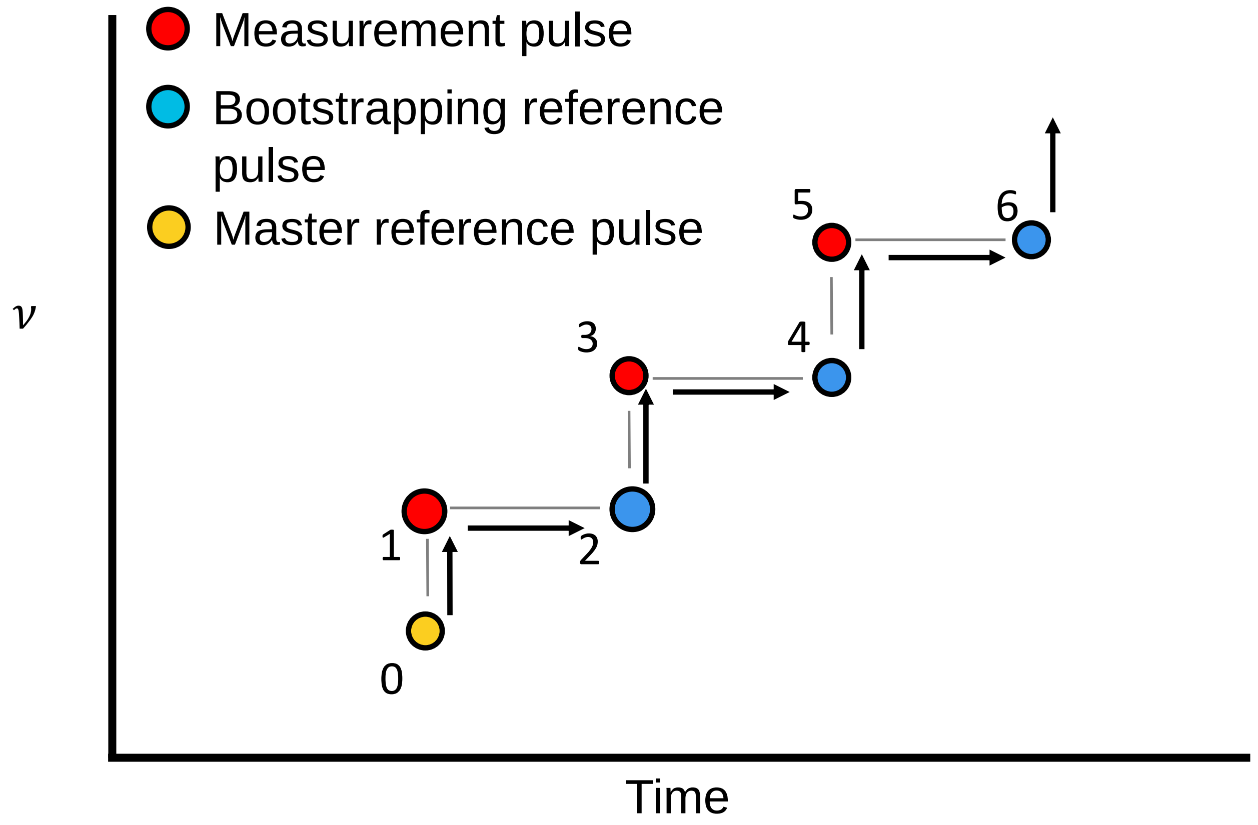

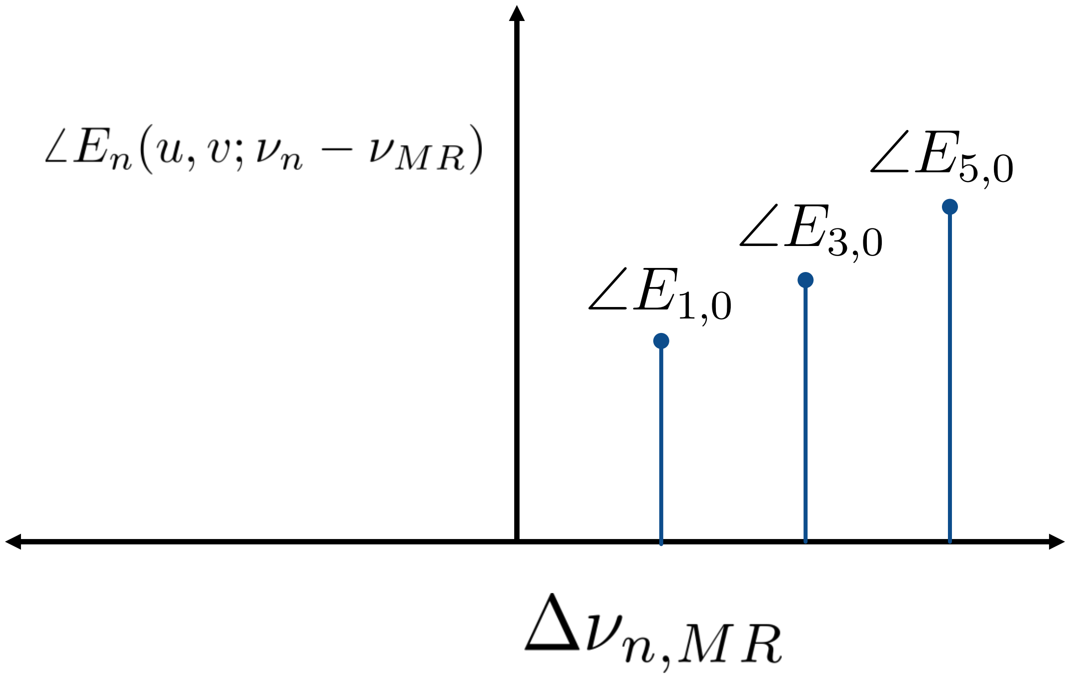

Wrapped range images: pilot-tone 3D imaging

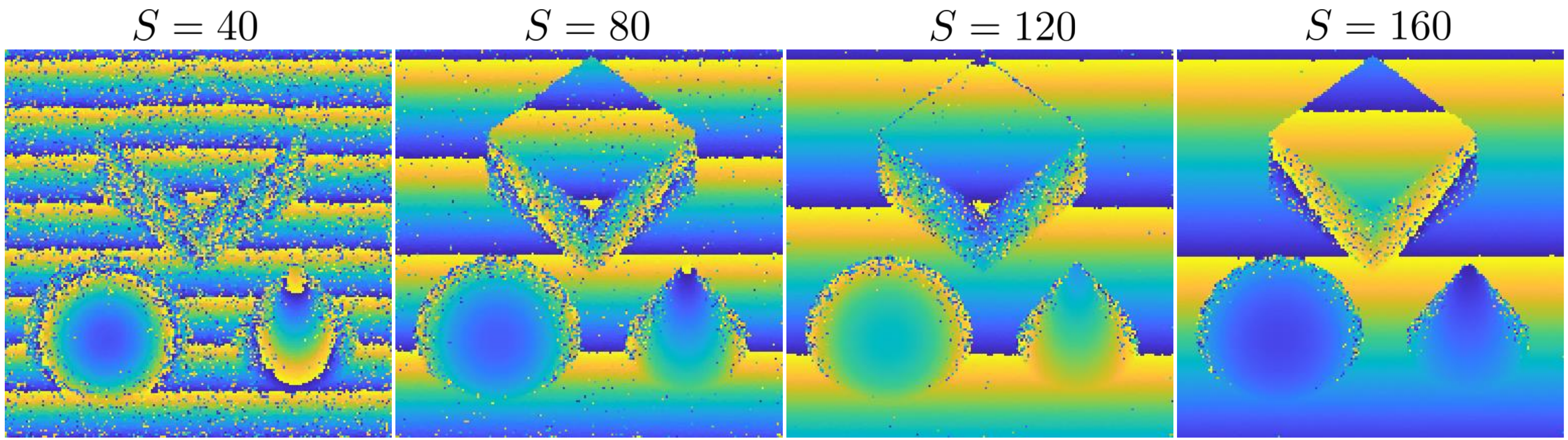

Pilot-tone images robust to object motion but feature range chatter over highly sloped facets

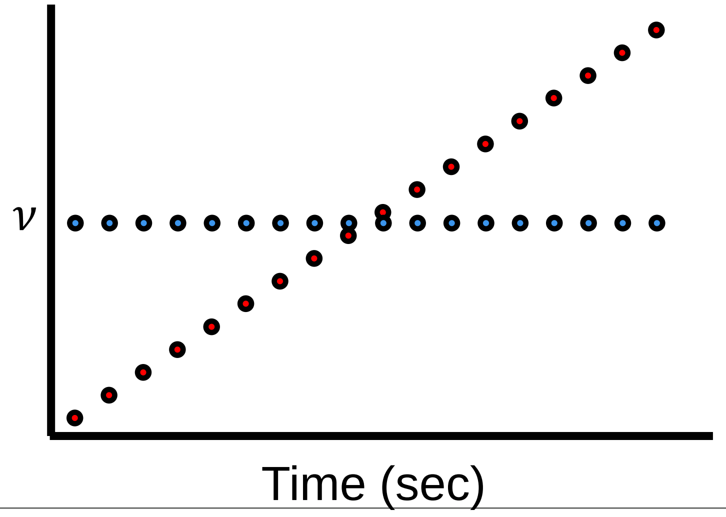

Wrapped range images: dual-tone 3D imaging

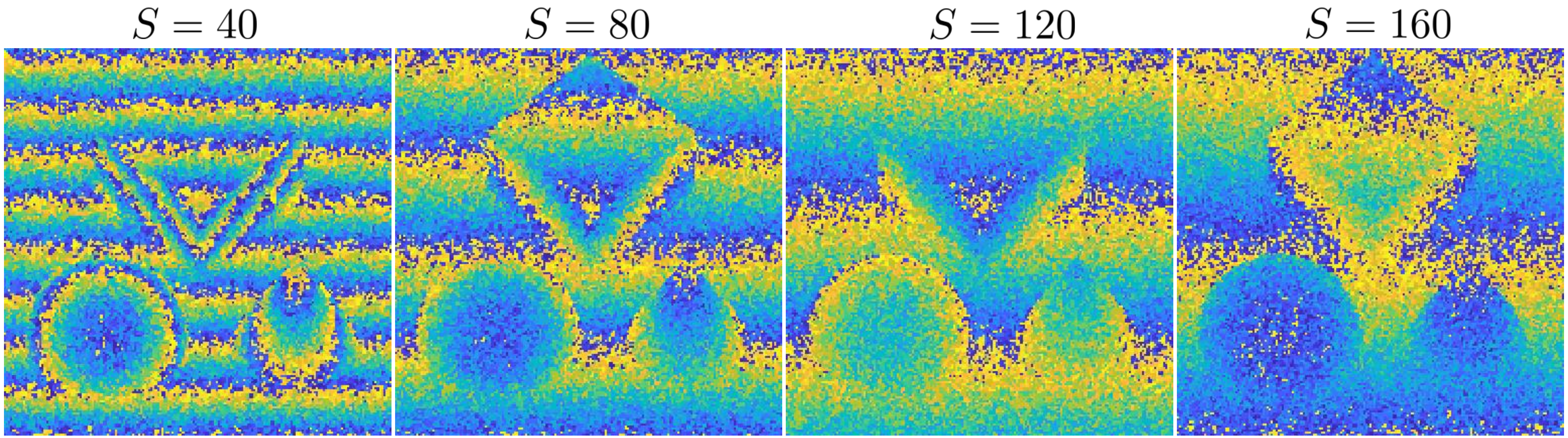

Dual-tone images feature consistent range errors over the image due to object motion

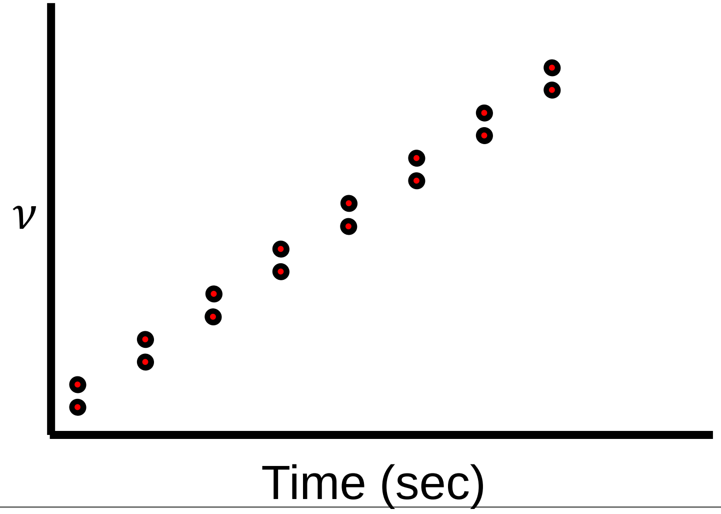

Wrapped range images: stairstep 3D imaging

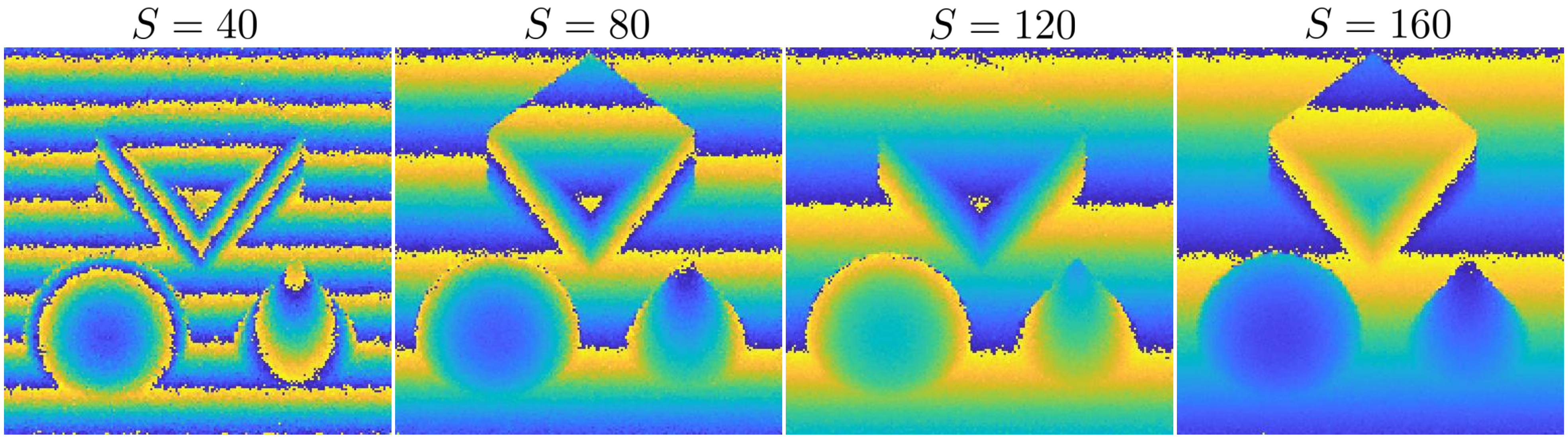

Stairstep images are relatively error free

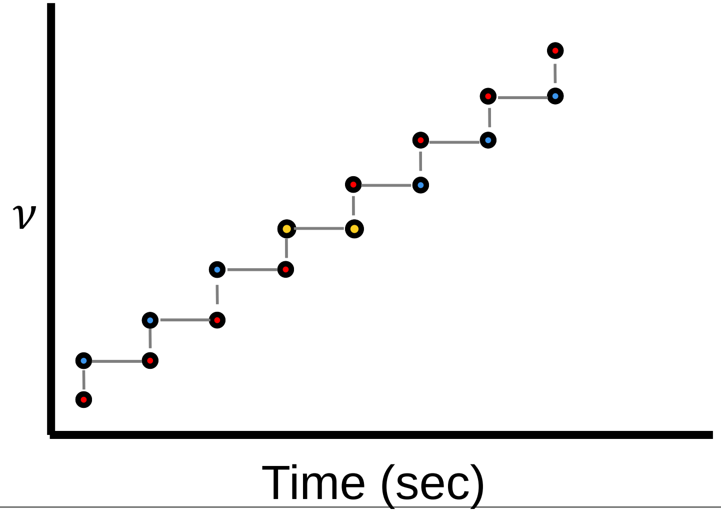

Quantitative results for wrapped range images

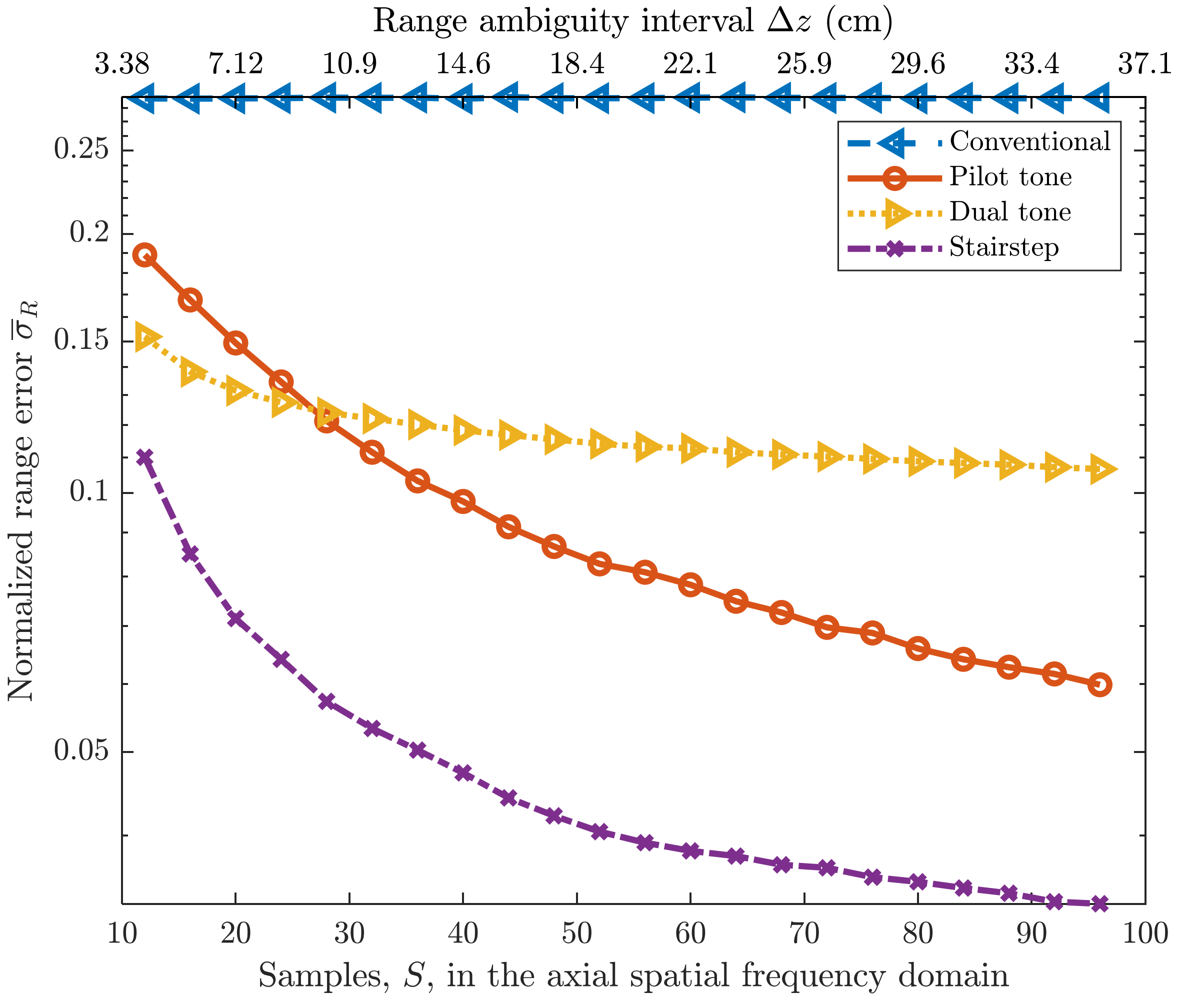

<u>Normalized Wrapped Range Image Error</u>

$$\overline{\sigma}_R = \left(\mathrm{std}_{u,v\in W(u,v)}\left\{R_e(u,v)\right\}\right)/\Delta z$$

$$R_e(u,v) = \mathrm{mod}\left[\hat{R}(u,v) - R(u,v) + \Delta z/2, \Delta z\right] - \Delta z/2$$

Range image — Truth range image

Stairstep 3D imaging performs the best given infinite SNR

Banet, M. T., Idris, A., & Fienup, J. R. (2023, October). Multiplexed, multi-wavelength 3D digital holographic imaging methods with range unwrapping. In *Unconventional Imaging, Sensing, and Adaptive Optics 2023* (Vol. 12693, pp. 12-24). SPIE.

Simulation trade space for unwrapped range images

- Three 3D imaging modalities
    - Pilot-tone 3D imaging
    - Dual-tone 3D imaging
    - Stairstep 3D imaging
- Keep bandwidth, $\Delta\nu$, constant and vary number of samples in optical frequency domain, S
- Enforce independent surface roughness realizations at each timestep

Maximum range discontinuity determines unwrapping performance

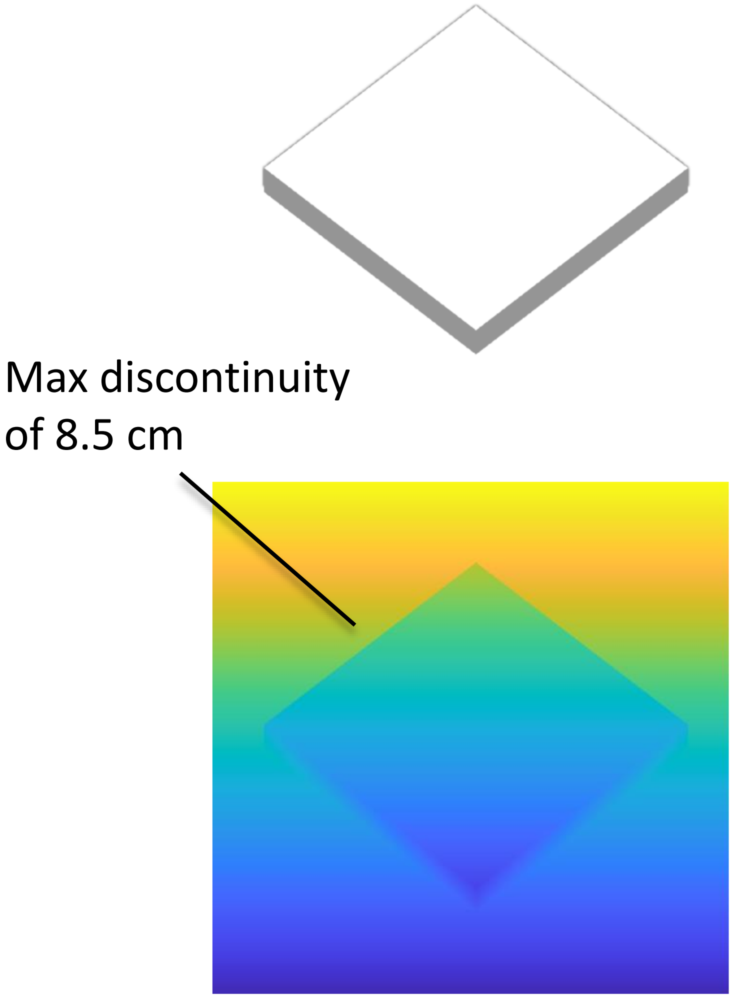

Wrapped range images: raised square plate

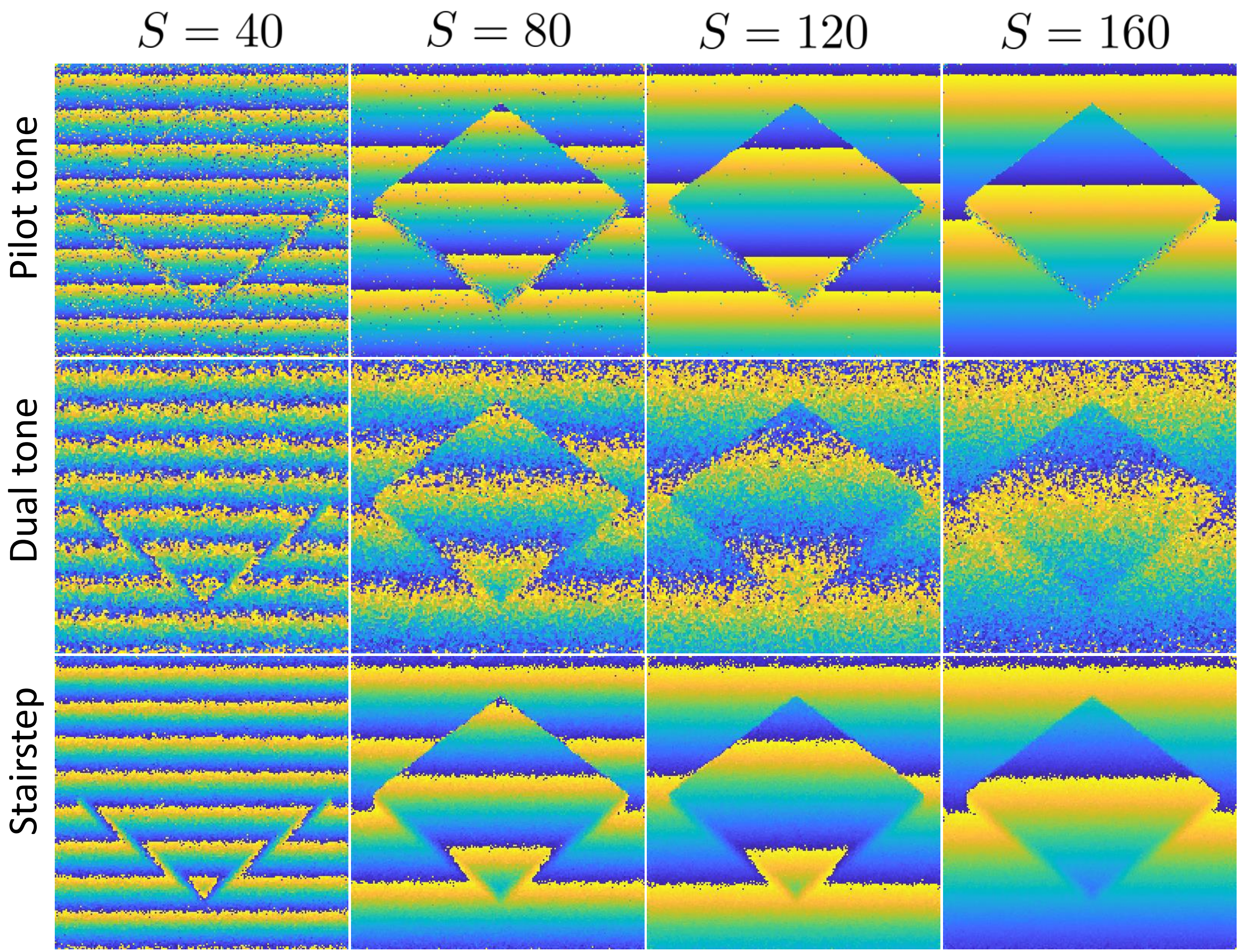

Unwrapped range images: raised square plate

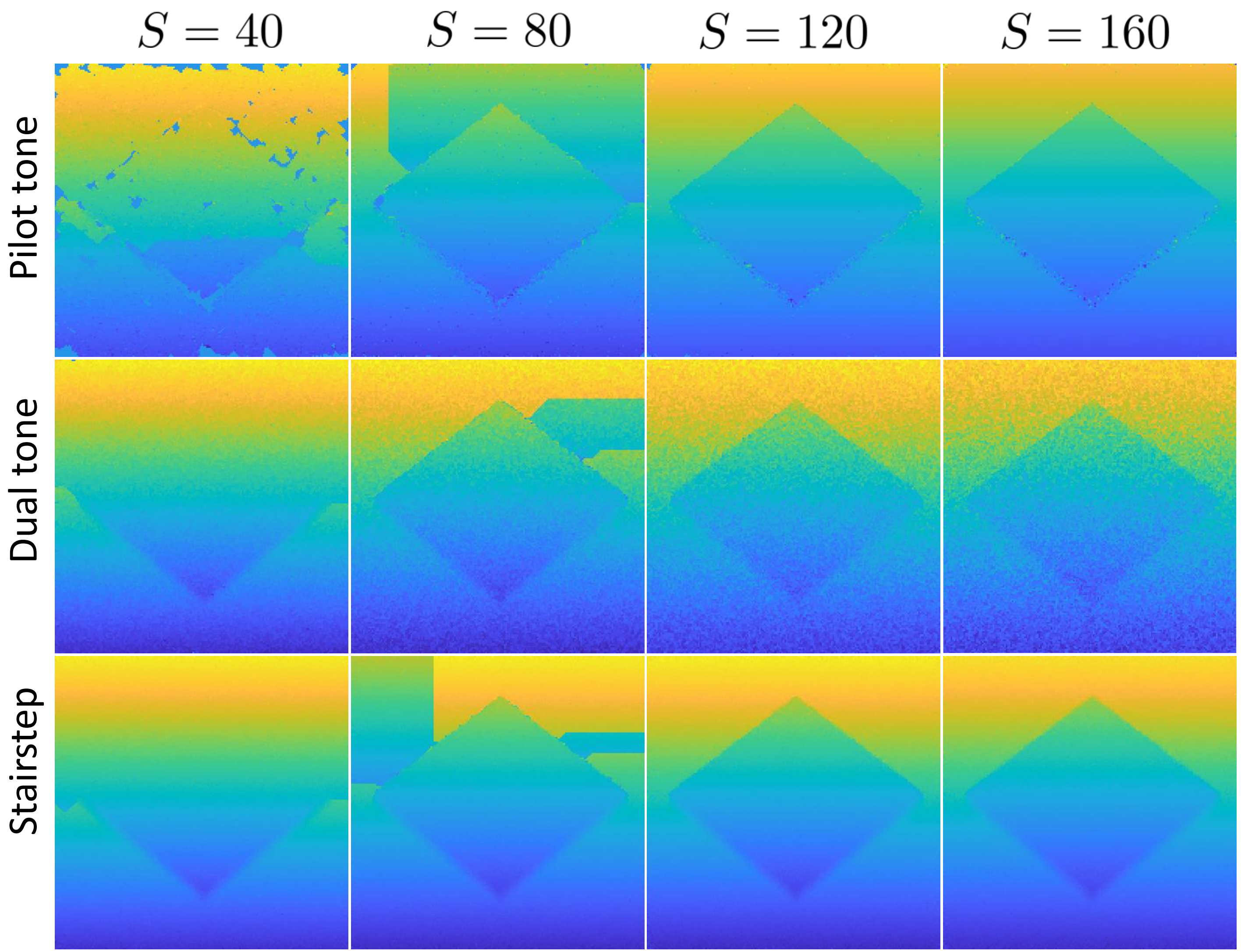

Quantitative results for unwrapped range images

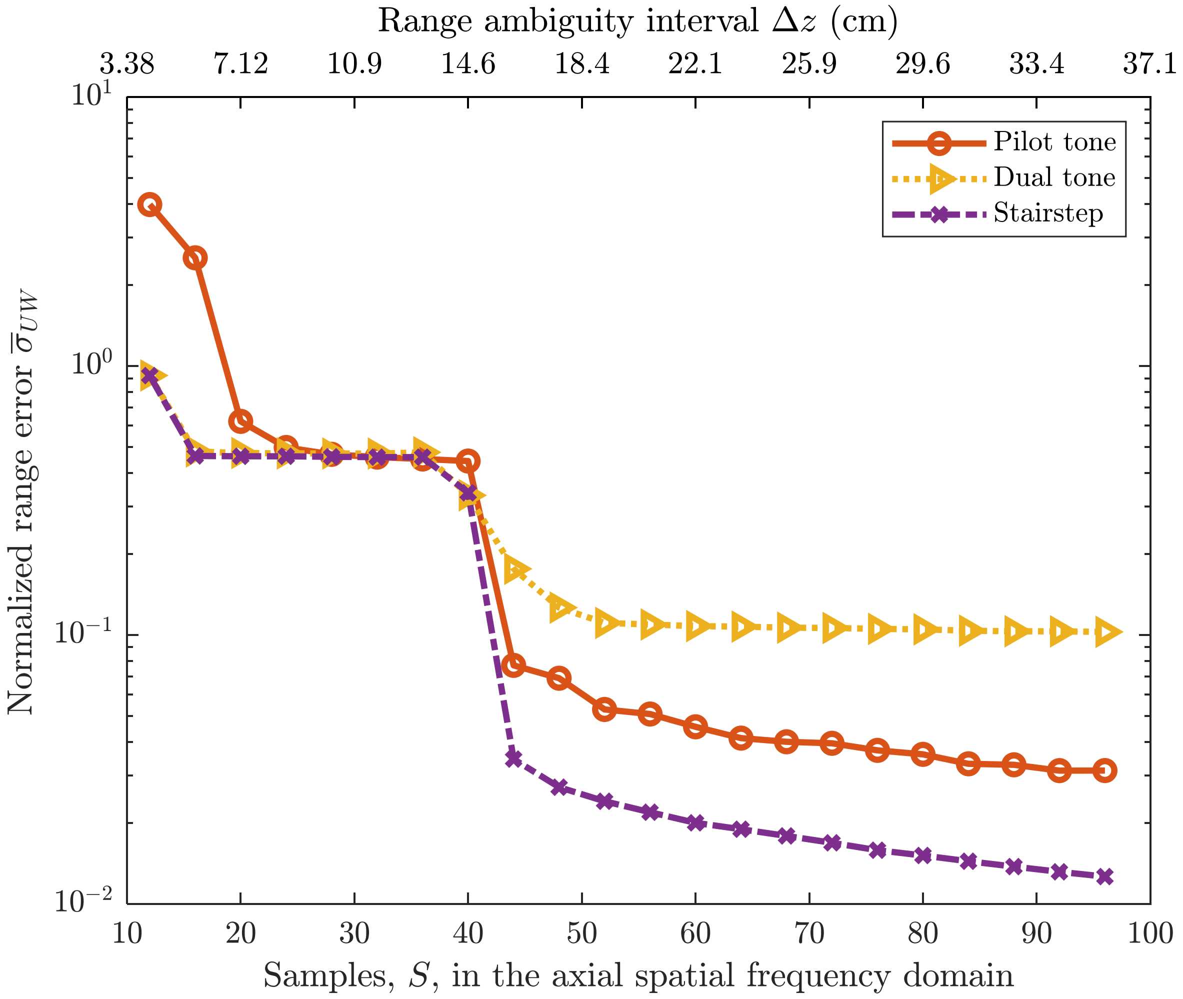

Normalized Unwrapped Range Image Error

$$\overline{\sigma}_{UW} = \left(\mathrm{std}_{u,v\in W(u,v)}\left[\hat{R}(u,v) - R(u,v)\right]\right)/\Delta z$$

Range image — Truth range image

Recall max discontinuity of 8.5 cm

Performance gets suddenly worse as Δz becomes less than twice the maximum range discontinuity

Banet, M. T., Idris, A., & Fienup, J. R. (2023, October). Multiplexed, multi-wavelength 3D digital holographic imaging methods with range unwrapping. In *Unconventional Imaging, Sensing, and Adaptive Optics 2023* (Vol. 12693, pp. 12-24). SPIE.

Signal-to-noise (SNR) model for pilot-tone and stairstep methods

Pilot-tone 3D imaging

- We vary the SNR of each 2D coherent image, $U(u, v; \nu)$, with variable SNR_{U_n}.
- Each frequency-difference image is formed by a **single conjugate product operation** between images from the chirped illuminator and the pilot tone
- Phase noise from the two component images adds which reduces the effective SNR of each frequency difference image by a factor of $\sqrt{2}$

$$E_n(u, v; \nu_n - \nu_p) = U_n U_{n,p}^*$$

$$\mathrm{SNR}_{E_n} = \frac{\mathrm{SNR}_{U_n}}{\sqrt{2}}$$

Stairstep 3D imaging

- We vary the SNR of each coherent image, $U(u, v; \nu)$, with variable SNR_{U_n}.
- Each frequency-difference image is formed by a **multiple conjugate product operations** that tie each coherent image to the master reference image
- Phase noise from the two component images adds which reduces the effective SNR of each frequency difference image by a factor of $\sqrt{2n}$

$$E_n(u, v; \nu_n - \nu_{mr}) = U_n U_{n,br}^* \exp(i\angle E_{n-1})$$

$$\mathrm{SNR}_{E_n} = \frac{\mathrm{SNR}_{U_n}}{\sqrt{2n}}$$

Simulation setup with picture of object

- Propagation distance, $z = 2$ km
- Circular aperture diameter, $D = 30$ cm
- Wavelength, $\lambda = 1.5$ µm

- Varied # of samples in frequency difference space, P
- Varied SNR of each 2D coherent image
- Kept total bandwidth $\nu_{max} - \nu_{min}$ constant

<u>Reflectance map</u>

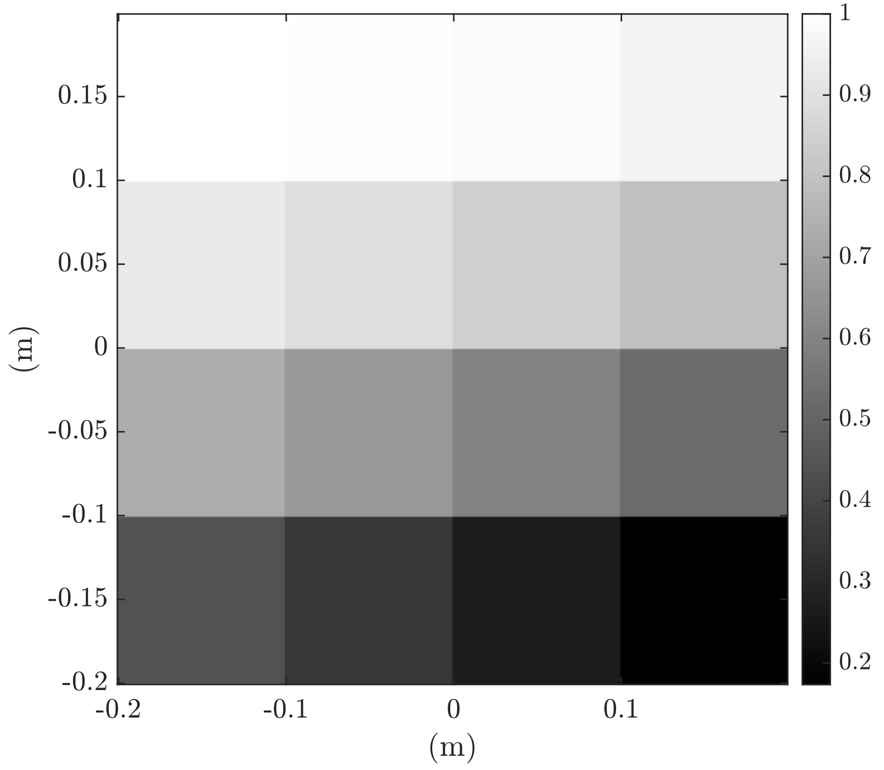

<u>Depth map</u>

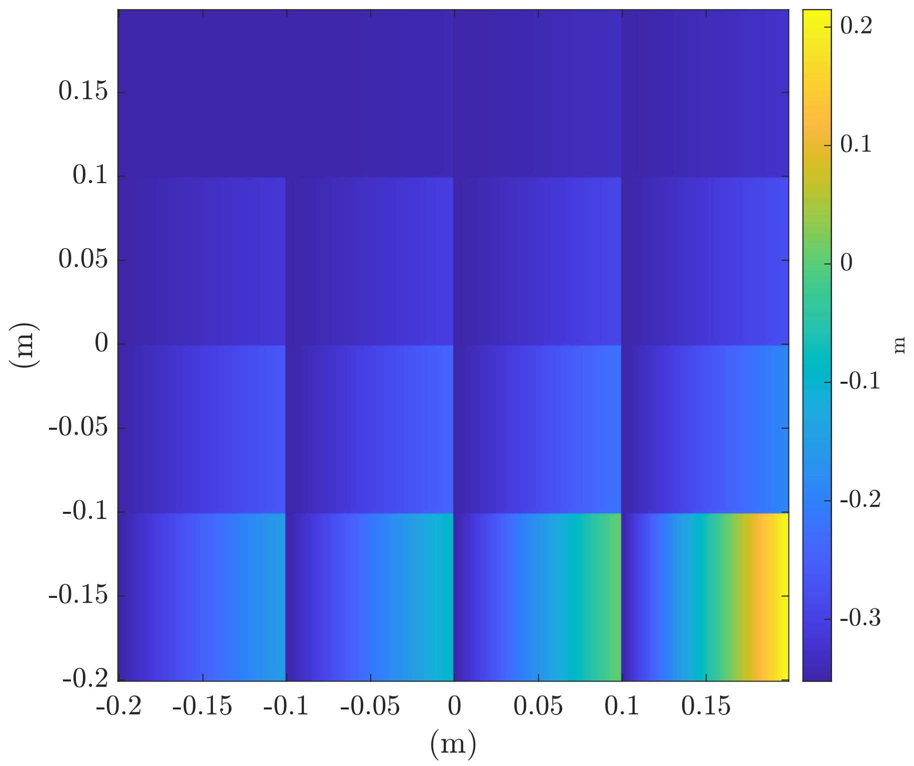

Results: Range images for $P = 20$ and $\mathrm{SNR}_{U_n} = 10$

Pilot tone range image

Stairstep range image

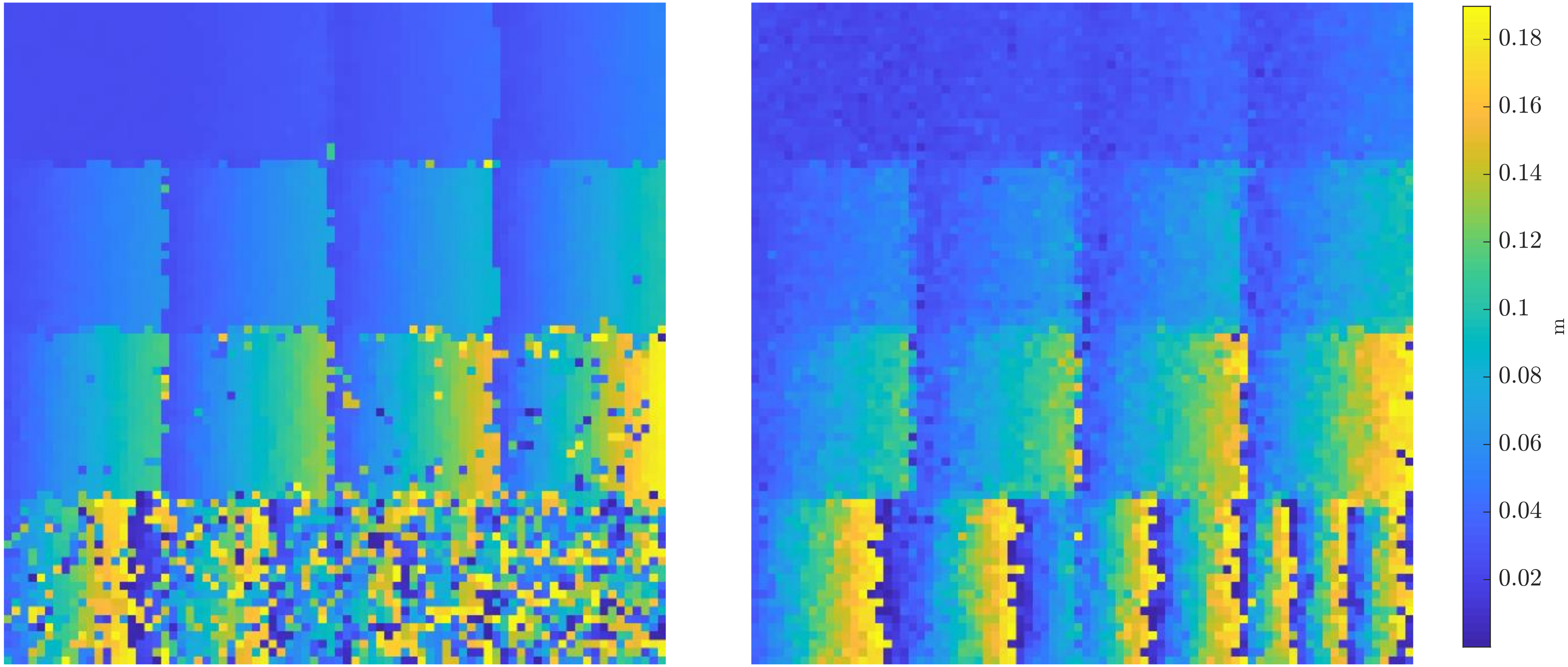

Results: Range image root-mean-square error (RMSE) vs. *P* for three different facet angles and various SNRs

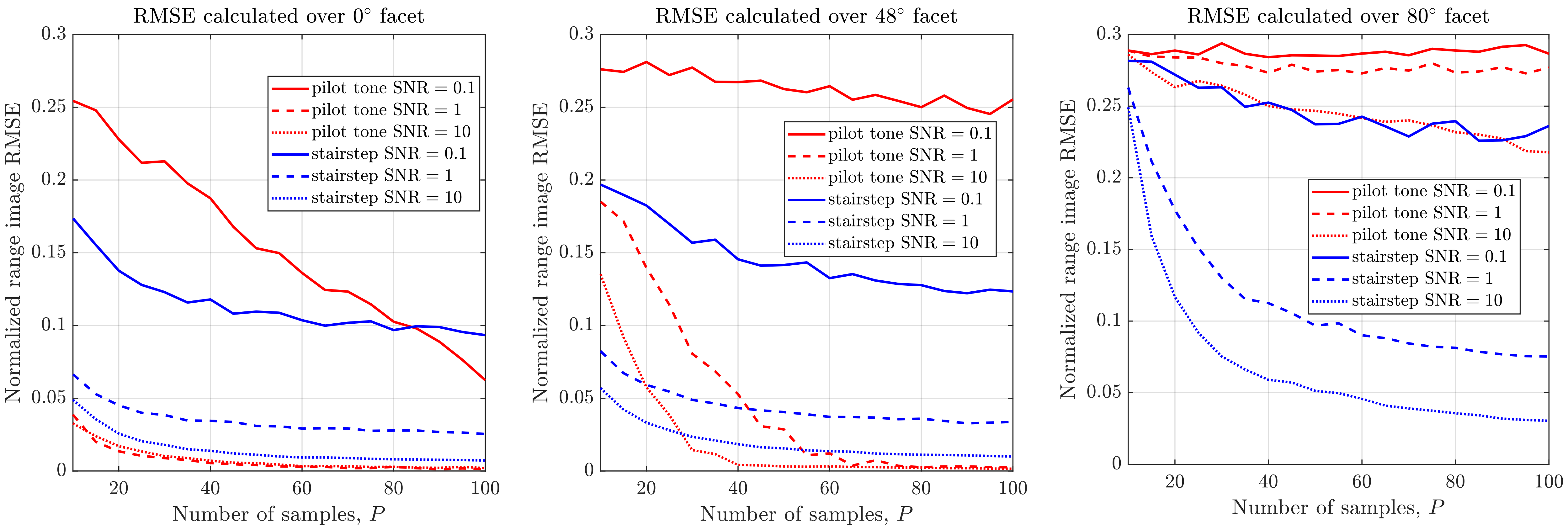

Banet, M. T., Wong, F., & Fienup, J. R. (2024, July). Stairstep versus pilot-tone 3D imaging: empirical signal-to-noise ratio studies. In Computational Optical Sensing and Imaging (pp. CF4A-2). Optica Publishing Group.

Results: Range image RMSE vs. P for three different facet angles and $\mathrm{SNR}_{U_n} = 10$

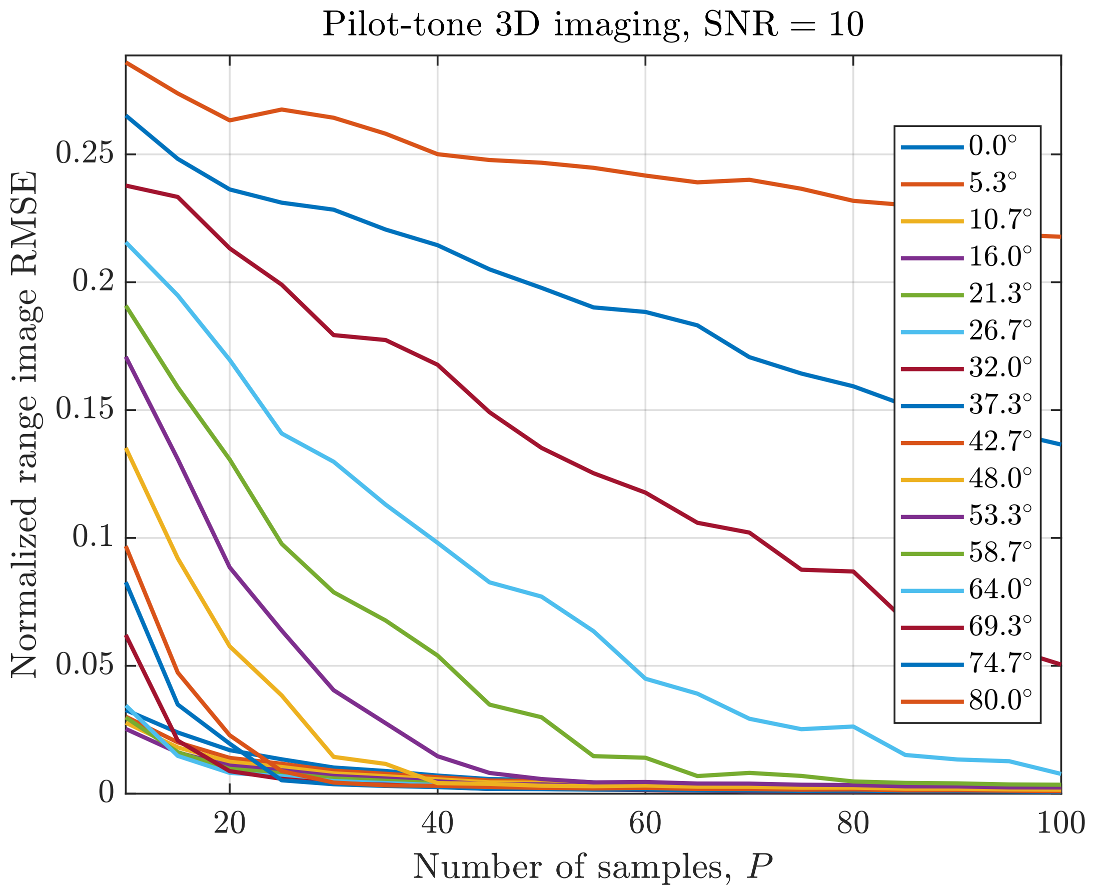

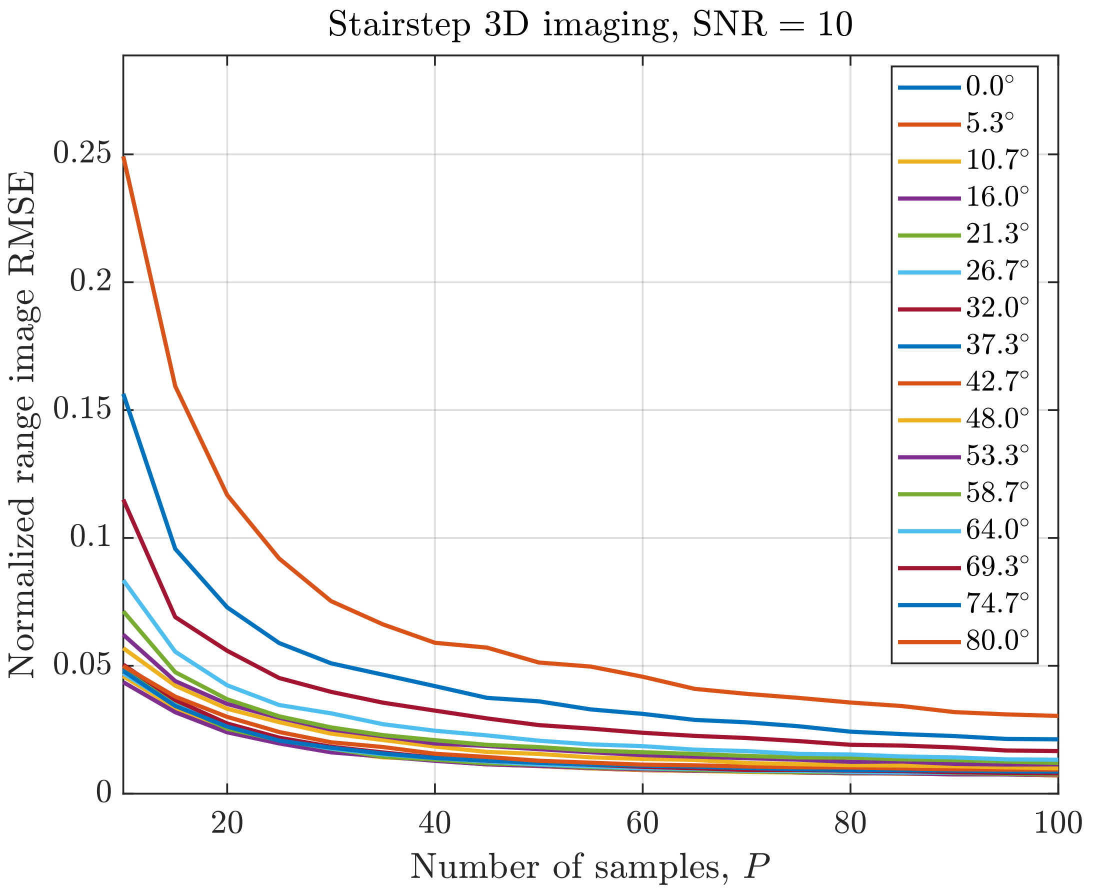

Banet, M. T., Wong, F., & Fienup, J. R. (2024, July). Stairstep versus pilot-tone 3D imaging: empirical signal-to-noise ratio studies. In Computational Optical Sensing and Imaging (pp. CF4A-2). Optica Publishing Group.

Conclusions

- Stairstep imaging provides better results for highly sloped facets of the object
- Pilot tone imaging generally outperforms stairstep imaging for objects with shallow slopes and practical SNRs (1-10)
- Range unwrapping is viable when range discontinuities are less than half the range ambiguity interval
- Adding illuminators adds enables more modalities for motion-compensated 3D imaging

Pilot tone range image

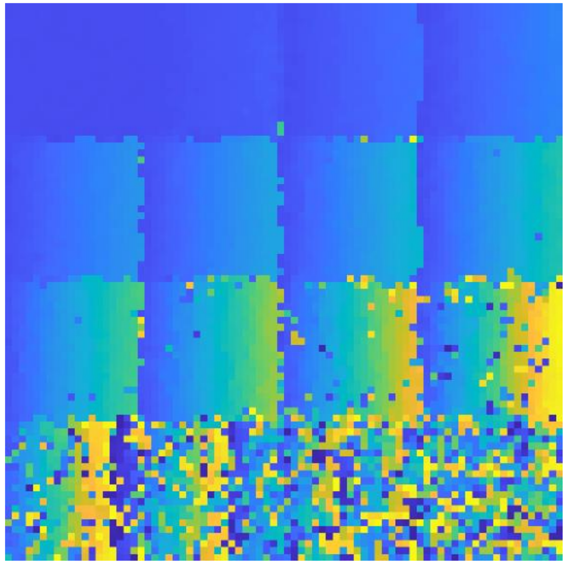

Stairstep range image

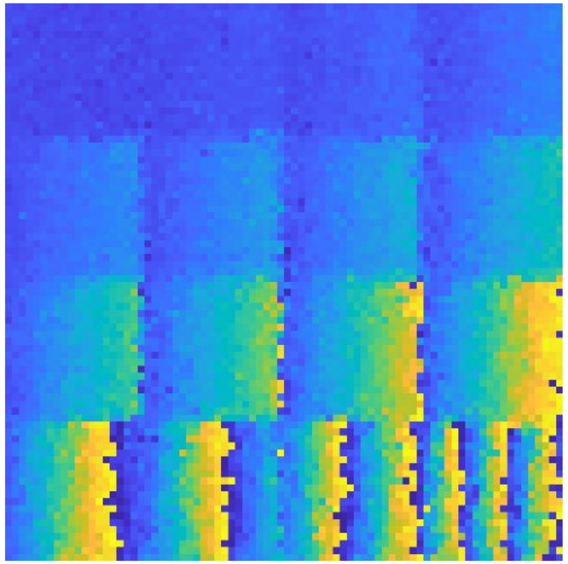

Future work

- Exploring a hybrid approach that can leverage the best qualities of both methods
- Fleshing out the theoretical SNR models for each method for more in-depth comparisons
- Exploring alternate methods to dual-tone imaging that might perform well for moving/vibrating objects
- **Researchers at MZA Associates Corporation and Dr. Fienup's group at the University of Rochester are continuing this work!**

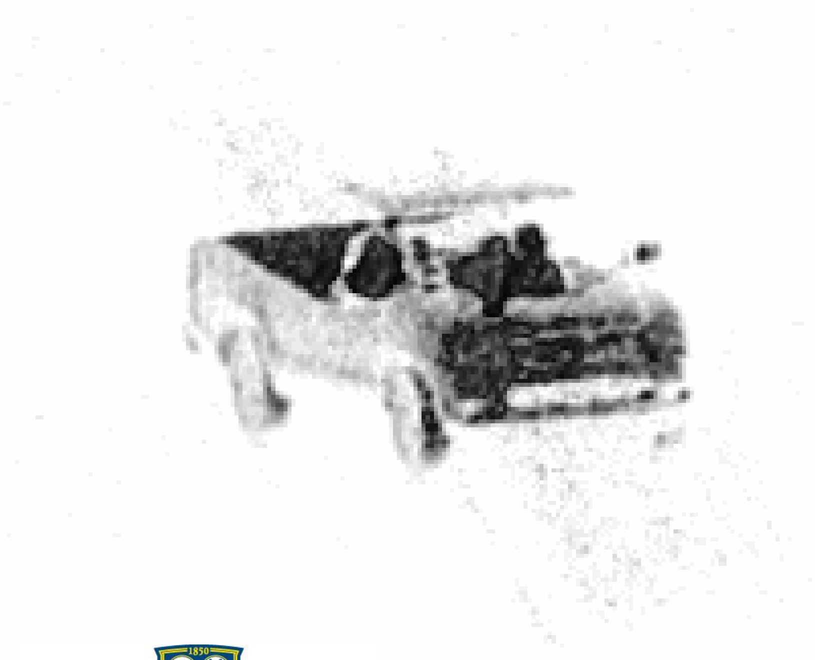

HAJIM SCHOOL OF ENGINEERING & APPLIED SCIENCES UNIVERSITY of ROCHESTER

MZA

Related work

- Phase difference imaging requires just two laser pulses of differing frequency (related to conjugate product images)

- 3D imaging with digital holography also enables 3D image reconstruction via sharpness metric maximization

Questions?

Phase difference imaging[1]

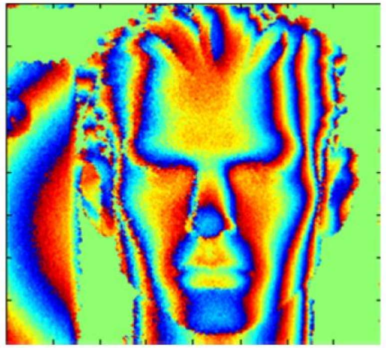

Motion-compensated 3D imaging[2]

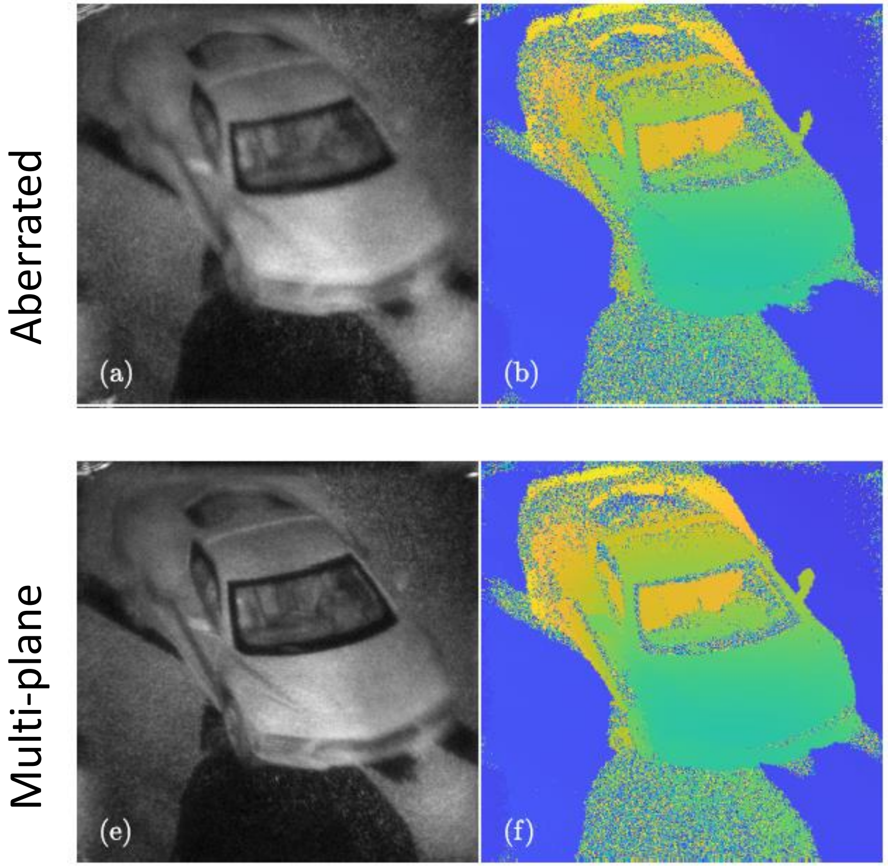

1. Marron, J. C., Kendrick, R. L., Thurman, S. T., Seldomridge, N. L., Grow, T. D., Embry, C. W., & Bratcher, A. T. (2010, April). Extended-range digital holographic imaging. In Laser Radar Technology and Applications XV (Vol. 7684, pp. 493-498). SPIE.
2. Banet, M. T., Fienup, J. R., & Krause, B. W. (2024). Demonstration of multi-plane sharpness metric maximization on motion-compensated, multi-wavelength 3D digital holographic field data. *Optics Letters*, *49*(3), 418-421.

Extra slides

Speckle correlation with variable wavelength

- Assume that transverse correlation of surface roughness profile is delta-correlated (safe to assume for most wave-optics grid sample sizes)
- Isolate speckle decorrelation effects due to **surface roughness,** neglecting decorrelation effects from diffraction, which can be modeled easily

Irradiance correlation versus $\Delta\lambda$ for $\bar{\lambda} = 1$ µm

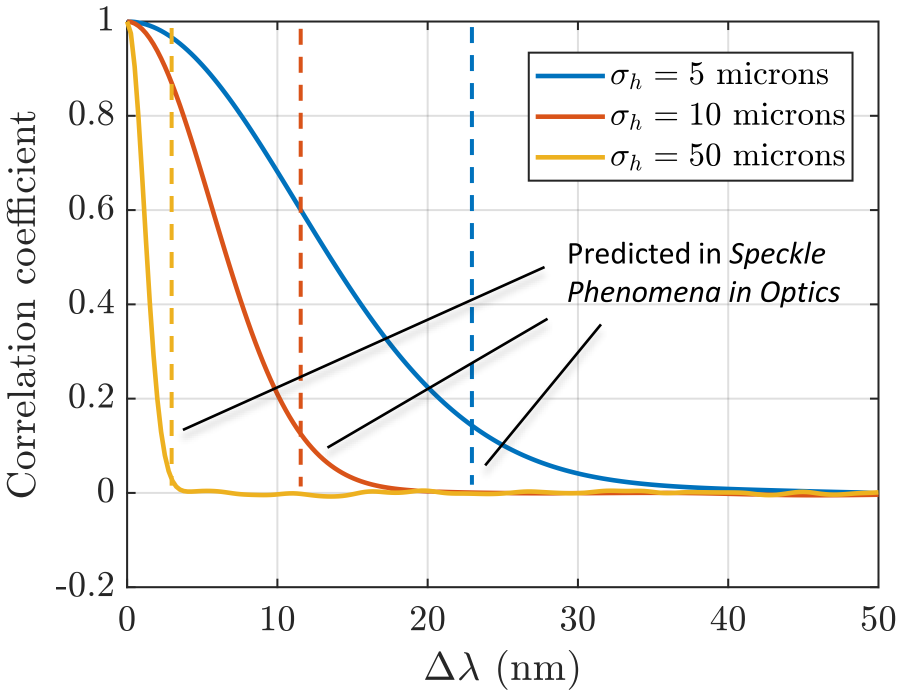

Reflective Samples	Enhancement (η)	Roughness (R_{rms})
Brushed aluminum	122.3	1.5 µm
Infragold®	89.9	9.4 µm
Sandblasted aluminum	67.7	2.3 µm
Graphite	37.3	3.5 µm
White paint	36.8	1.7 µm
Spectralon®	13.8	Unprofiled
Transmissive Sample		
White paint	56.4	1.7 µm

Burgi, K., Ullom, J., Marciniak, M., & Oxley, M. (2016). Reflective inverse diffusion. Applied Sciences, 6(12), 370.

$$|\Delta\lambda| \geq \frac{1}{2\sqrt{2\pi}} \frac{\bar{\lambda}^2}{\sigma_h}$$

$1/e^2$ decorrelation point according to Eq. (6.47)
(*Speckle Phenomena in Optics: Theory and Applications*, 2nd Ed.)

Practical implications of speckle correlation with variable wavelength

- Most modeling involves quasi-monochromatic light or **narrow fractional bandwidths** for which **surface roughness effects** are mostly unchanging
  - Long range 3D imaging: $\Delta\nu \sim 30$ GHz or $\Delta\lambda \sim 0.1$ nm at $\bar{\lambda} = 1$ µm

- For narrow fractional bandwidths, object plane modeling can include a **coarse depth phasor** for diffractive effects and **circular complex Gaussian random numbers** for surface roughness effects

$$\underbrace{U_{1,\perp}(x,y)}\,\underbrace{\exp[i2kZ_d(x,y)]}\,\underbrace{[\mathcal{N}(0,0.5)+i\mathcal{N}(0,0.5)]}$$

Models object reflectance — Models diffractive effects — Models surface roughness

Irradiance correlation versus $\Delta\lambda$ for $\bar{\lambda} = 1$ µm

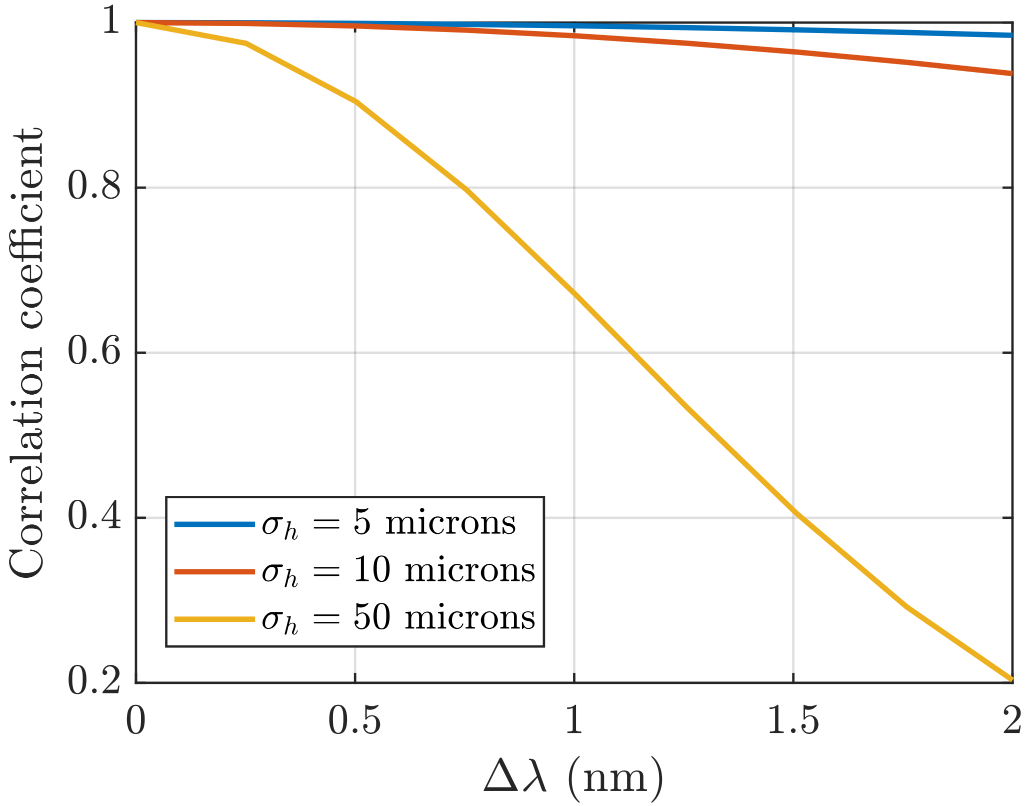

Fractional bandwidth: $\Delta\lambda/\bar{\lambda}$